Experimental Mathematics
Publication details, including instructions for authors and subscription information:
http://www.informaworld.com/smpp/title~content=t926086164

Geometrical Models for Substitutions

Pierre Arnoux[a]; Julien Bernat[b]; Xavier Bressaud[c]
[a] Institut de Mathématiques de Luminy, Marseille Cedex 09, France [b] IUFM de Lorraine et Institut Elie Cartan, Vandoeuvre-lés-Nancy Cedex, France [c] Institut de Mathématiques de Toulouse, Université Paul Sabatier, Toulouse Cedex 9, France

Online publication date: 09 March 2011

To cite this Article Arnoux, Pierre , Bernat, Julien and Bressaud, Xavier(2011) 'Geometrical Models for Substitutions', Experimental Mathematics, 20: 1, 97 — 127
To link to this Article: DOI: 10.1080/10586458.2011.544590
URL: http://dx.doi.org/10.1080/10586458.2011.544590

Experimental Mathematics, 20(1):97–127, 2011

ISSN: 1058-6458 print
DOI: 10.1080/10586458.2011.544590

Taylor & Francis
Taylor & Francis Group

Geometrical Models for Substitutions

Pierre Arnoux, Julien Bernat, and Xavier Bressaud

CONTENTS

We consider a substitution associated with the Arnoux–Yoccoz interval exchange transformation (IET) related to the tribonacci substitution. We construct the so-called stepped lines associated with the fixed points of the substitution in the abelianization (symbolic) space. We analyze various projections of the stepped line, recovering the Rauzy fractal, a Peano curve related to work in [Arnoux 88], another Peano curve related to the work of [McMullen 09] and [Lowenstein et al. 07], and also the interval exchange transformation itself.

1. INTRODUCTION

1.1. Historical Background

After the classification by Thurston of the automorphisms of surfaces and the definition of pseudo-Anosov automorphisms of surfaces, one sought to determine the possible dilation coefficients of such automorphisms; at the time, the only known examples were lifts of toral automorphisms, with quadratic coefficients.

One of the earlier nontrivial examples was a cubic one [Arnoux and Yoccoz 81], whose dilation coefficient was the real root λ of the tribonacci polynomial $X^3 - X^2 - X - 1$; it was found as an application of Veech's method, by exhibiting a particular interval exchange transformation on the unit circle that is conjugate to its first return map on an interval of length $\alpha = 1/\lambda$ (see Section 3.1 for details).

Around the same time, it was shown in [Rauzy 82] how to give geometric models of a particular type of substitution dynamical system as a rotation on the torus, by projecting the stepped line corresponding to the fixed point of the substitution. The first example, concerning the tribonacci substitution on three letters $a \mapsto ab$, $b \mapsto ac$, $c \mapsto a$, also involved the tribonacci polynomial (the characteristic polynomial of the abelianization matrix); the two systems were soon shown to be measurably conjugate, and even semiconjugate by a continuous, onto, measure-preserving map from the circle to the torus (a Peano curve) [Arnoux 88]. Indeed, the interval exchange transformation, because of the property of self-induction,

2000 AMS Subject Classification: 37B10, 37E05

Keywords: Interval exchange transformations, Rauzy fractals, substitutive dynamical systems, Peano curves

was easily seen to be measurably conjugate to the symbolic system defined by the substitution. This example was a special case of a property, proved in [Fathi 88], of semiconjugacy of a pseudo-Anosov map to the toral automorphism defined by the homology in the hyperbolic case, where the homology matrix has no eigenvalue of modulus one.

This example was also considered in [Sirvent 97, Sirvent 00, Messaoudi 00], whose authors considered various properties. More recently, McMullen built from this example, by lifting the orbit of 0 to $\mathbb{Q}(\lambda)$ viewed as $\mathbb{Q}^3$, a curious stepped curve with self-similarity properties (a "deterministic Brownian motion") whose vertices completely fill a slice of a 3-dimensional lattice contained between two parallel planes; see [McMullen 09]. This curve was studied in detail in by Lowenstein, Poggiaspalla, and Vivaldi in [Lowenstein et al. 07].

However, the methods involved are ad hoc and difficult to generalize; they leave a number of open problems: the partition used for the coding of the interval exchange transformation is only generating in measure, almost everywhere, not everywhere; the reciprocals of the eigenvalues, which should always be present for a self-induced interval exchange transformation (because of the preservation of the symplectic form on the homology by the related pseudo-Anosov map) disappear at the symbolic level; and there is at the moment no systematic way to reconstruct the interval exchange transformation from the substitution (in particular, the projection method seems to produce only group translation factors, not interval exchanges transformations). There is also a periodic behavior of order 3 linked to the permutation of the separatrices of the singular point by the pseudo-Anosov map, which is hidden in several constructions, as in the paper [Lowenstein et al. 07], which considers self-similarity by the cube of the tribonacci number.

In this paper, we present a complete study of this example, recovering all these properties in a more systematic way, and giving some insight into the structure of the interval exchange transformation. The basic tool is a partition into nine intervals that is finer than the partition by continuity intervals, hence generating, and adapted to the substitution. The linear map associated with the substitution admits as characteristic polynomial the product of the tribonacci polynomial, its reciprocal polynomial, and the polynomial $X^3 - 1$. With this substitution are associated some stepped lines in $\mathbb{R}^9$, coming from infinite periodic points for the substitution; this gives a unified setting from which we can obtain all the geometric objects described above (interval exchange transformation, Rauzy fractal, McMullen curve). By projecting these stepped lines onto the various invariant subspaces and using renormalization when needed, we recover the geometric models for this substitution as a toral translation or interval exchange transformation, and the McMullen curve. We get a much better understanding of this dynamical system, which should be viewed as defined not on a circle, but on the disjoint union of three intervals.

This study is an example of application of some general properties of substitutions that allows one to recover all classical properties in a systematic way and to find several new ones. It raises a number of open questions.

Remark 1.1. This example has been much studied recently from a different viewpoint. As we explained above, the suspension of the interval exchange gives a measured foliation on a surface of genus 3 that is the stable foliation of a pseudo-Anosov map; the unstable measured foliation of this map is well defined, up to a constant, and this defines a quadratic differential on the surface (up to the action of the geodesic Teichmüller flow). This quadratic differential defines uniquely a periodic orbit for the Teichmüller flow on the modular space of quadratic differentials; it also defines a Teichmüller disk for the natural action of $\mathrm{SL}(2,\mathbb{R})$.

The stabilizer of the initial quadratic differential, the "Veech group," is the subject of four recent papers. It is obviously nontrivial, since it contains the derivative of the pseudo-Anosov map. In [Hubert and Lanneau 06], the authors prove that this Veech group does not contain any parabolic element; the authors of [Hubert et al. 09] complete the analysis: they prove that the Veech group is not cyclic, since it contains another hyperbolic element corresponding to a different stable foliation, and the Teichmüller disk is dense in the largest possible subspace (the hyperelliptic locus of the connected component of the stratum that contains it), a behavior that is very different from the quadratic case. In [Bowman 08], a new description of the quadratic differential is given in terms of Delaunay polygons; and in [Nipper 08], the author shows that this quadratic differential does not satisfy Veech's dichotomy: there is an uncountable set of minimal but not uniquely ergodic directions.

1.2. Outline of the Paper

We study the properties of several objects related to the interval exchange transformation defined in [Arnoux and Yoccoz 81], using two general constructions for substitutions.

Section 2 is basic for the rest of the paper, and gives these constructions. We define stepped lines associated with words and substitutions; for a given substitution σ with abelianization matrix M_σ, we show that the projection to the contracting space of M_σ of a canonical stepped line associated with σ is a bounded set. Its closure, called the Rauzy fractal, is a union of a finite number of pieces indexed by the alphabet, with the action of a pseudogroup of translations defined on each piece (it is a map if the pieces are disjoint). If instead we project to the expanding space the finite curves corresponding to $\sigma^n(a)$, we obtain an unbounded sequence of sets, which can be renormalized to converge to a self-similar curve. The Rauzy fractal and the renormalized curve are both solutions of two graph-directed iterated function systems that are dual in a precise sense.

In Section 3 we define the basic objects of this paper: the interval exchange transformation T, a partition for the domain of T (this partition is into nine intervals, and is the basis of all results of this paper), and a related substitution σ on nine letters, whose characteristic polynomial is the product of the tribonacci polynomial, its reciprocal polynomial, and the polynomial $X^3 - 1$. This substitution has several factors, including, in a very natural way, the tribonacci substitution. The abelianization matrix of the substitution can split in a dynamical way, with a stable space E_s, an unstable space E_u, and a neutral space E_n, corresponding to the eigenvalues of modulus smaller than, larger than, or equal to 1. It can also split in an arithmetic way, in the tribonacci space E_T, the "antitribonacci" space $E_{\bar{T}}$ and the neutral space, corresponding to the three factors of the characteristic polynomial on the integers. Note that E_T, $E_{\bar{T}}$, and E_n are rational spaces, for which we can take basis vectors with integral coordinates, while E_s and E_u are not. The space E_n itself splits into the direct sum of E_I, the line associated with eigenvalue 1, and E_j, the plane associated with eigenvalues j and $\bar{j}$. When we project onto one of these subspaces, it should be understood that unless otherwise stated, we project along the supplementary space.

Our main object of study will be the *stepped line* associated with a periodic point of the substitution by taking the abelianization of the prefixes. We will apply the results of Section 2 to the substitution defined in Section 3, and obtain several objects that shed new light, in particular, on the nature of this interval exchange transformation, which should not be considered as defined on a circle, but on three disjoint intervals, which have a natural interpretation on the surface obtained as a suspension of the interval exchange transformation.

In Section 4, we shall project onto the space $E_{T,s} = E_T \cap E_s$ and recover the Rauzy fractal in a natural way. By projecting onto $E_{\bar{T},s} \oplus E_j$, we obtain three intervals; by projecting these three intervals in an appropriate way (not along E_j), we recover the initial interval exchange transformation. We can also project onto the complete stable space E_s; we obtain a bounded set. If we choose correctly an appropriate direction of projection, the image turns out to be a continuous curve in $\mathbb{R}^3$, of Hausdorff dimension 2. This curve projects in a one-to-one way onto $E_{\bar{T},s}$ (it is strictly increasing in this direction), and it also projects one-to-one, except for a set of measure 0, onto the plane $E_{T,s}$; it is, in fact, the graph of the Peano curve given by the semiconjugacy of the interval exchange transformation to a torus rotation, which appears naturally by projection.

In Section 5, we project to E_n, and prove that the projection of the stepped line is a discrete set, whose projection to E_I is unbounded but whose projection onto E_j is finite, consisting of three points; these three points correspond to a partition into three intervals of the domain of the interval exchange transformation. They provide a more conceptual way to recover the results of Section 4.

In Section 6, we consider the projection to the unstable space, and obtain by renormalization a set of finite curves of high Hausdorff dimension. We will also consider the projection to the space $E_{\overline{T}}$. We obtain a discrete set contained in a slice of $\mathbb{Z}^3$; the projection of this set to a plane is an approximation of the McMullen curve, which has the same renormalization. If we use also the space E_j, we can obtain exactly the McMullen curve as a projection of the stepped line. We can in this way recover the results of [Lowenstein et al. 07] in a systematic way.

In Section 7, we use the order structure given by the interval exchange transformation to define a new substitution dual to the first one, for which we can also study fixed points and the projections to various spaces. Note that the definition of the dual substitution is not trivial; the matrix of this dual substitution is uniquely defined as the transpose of the matrix of the initial substitution. But this matrix is not sufficient to define a substitution: it defines only the abelianization of the images of letters. To recover the ordering of the words, we need to use the order structure on the circle and the hierarchy of tilings given by the induction. In the general case, in which there is no natural order structure on the underlying space, the definition of a dual substitution is unclear. In the present case, it appears that the renormalized curves (projections of the stepped lines onto the unstable spaces) converge to

the fractals defined in Section 4. This is not completely surprising: changing the substitution to its dual is a first transposition, and changing from stable to unstable space entails a second transposition, which gives back the initial situation.

In Section 8, we make some remarks and present some open questions; in particular, we briefly discuss a flat structure on a surface of genus 3 associated with the interval exchange transformation; complete consideration of this surface would have lengthened this paper too much, but it underlies a large part of this work.

In the appendix (Section 9) we give a proof of some computational results used in the paper.

2. SUBSTITUTIONS AND GEOMETRIC MODELS

2.1. Substitution Dynamical Systems and Coding

Given a finite set $\mathcal{A}$ (the *alphabet*), a substitution on the alphabet $\mathcal{A}$ is a nonerasing morphism on the free monoid $\mathcal{A}^*$; it is completely defined by a map $\mathcal{A} \to \mathcal{A}^*$ that sends each letter to a nonempty word. Such a substitution σ is *primitive* if there exists n such that for every letter i, the word $\sigma^n(i)$ contains all letters of the alphabet. Primitive substitutions have a finite number of periodic points that are infinite sequences; the closure of the orbit under the usual shift map of any of these periodic points defines the symbolic dynamical system (Ω_σ, S) associated with the substitution. In this paper, we will deal only with primitive substitutions.

For a dynamical system (X, T) and a finite partition of X, $\mathcal{I} = \{I_i \mid i \in \mathcal{A}\}$, we define the *coding function* $\nu_\mathcal{I} : X \to \mathcal{A}$ by $\nu_\mathcal{I}(x) = i$ if $x \in I_i$, and we define the *itinerary* of a point $x \in X$ under T with respect to the partition $\mathcal{I}$ as the sequence $\big(\nu_\mathcal{I}(T^n x)\big)_{n\in\mathbb{N}}$. We will denote by $\varphi_\mathcal{I}$ the map that sends a point to its itinerary.

If A is a subset of X, and $x \in A$, we define the first-return time of x as $n_x = \inf\{n \in \mathbb{N}^* \mid T^n(x) \in A\}$ (it is infinite if the orbit of x does not return to A; this will not occur in the cases we consider). If the first-return time is finite for all $x \in A$, we define the induced map of T on A (or first-return map) as the map $x \mapsto T^{n_x}(x)$, and we denote this map by T_A.

Substitutions can be used to define symbolic dynamics for self-induced dynamical systems; more precisely:

Definition 2.1. Let (X, T) be a dynamical system, let σ be a substitution on the alphabet $\mathcal{A}$, and let $\mathcal{I} = \{I_i \mid i \in \mathcal{A}\}$ be a partition of X indexed by $\mathcal{A}$. We say that the dynamical system has σ-structure with respect to the partition $\mathcal{I}$ if there exist a subset $A \subset X$ and a bijection $h : X \to A$ such that:

1. The map h conjugates T to T_A: $T = h^{-1} \circ T_A \circ h$.
2. The first-return time, denoted by n_i, is constant on each set $J_i = h(I_i)$.
3. The sets $T^k(J_i)$, for $i \in \mathcal{A}$ and $0 \le k < n_i$, form a partition that refines the partition $\mathcal{I}$.
4. For $x \in J_i$, the finite coding $\big(\nu_\mathcal{I}(T^k x)\big)_{0\le k<n_i}$ with respect to the partition $\mathcal{I}$ is given by the word $\sigma(i)$.

If a system has σ-structure with respect to a partition, it is semiconjugate (by the itinerary map $\varphi_\mathcal{I}$) to the symbolic dynamical system associated with σ. If the sequence of partitions obtained by iterating the map h is generating (for example, if the diameter of the elements of this sequence of partitions tends to 0), this semiconjugacy $\varphi_\mathcal{I}$ is in fact one-to-one. In this paper, we will explore some examples of dynamical systems with σ-structure for a substitution.

To a substitution σ, we can associate the occurrence matrix $M_\sigma = (m_{i,j})_{i,j\in\mathcal{A}}$ indexed by $\mathcal{A}$, where $m_{i,j}$ is the number of occurrences of i in $\sigma(j)$. A substitution σ is primitive if and only if M_σ is primitive in the usual sense of matrices. In that case, the classical Perron–Frobenius theorem applies, and the matrix has a dominant eigenvalue, and an associated positive eigenvector.

2.2. Prefix Automaton

Let u be an infinite periodic point for the substitution σ, and let $u_1 \dots u_n$ be the prefix of length n of u. Since we can find v such that $u = \sigma(v)$, we can write $u_1 \dots u_n = \sigma(V)P_0$, where P_0 is a strict suffix of $\sigma(a_0)$ and Va_0 is a prefix of v; we can iterate the process, and find a sequence $P_0, P_1, \dots, P_k$ of prefixes of images of letters such that $u_1 \dots u_n = \sigma^k(P_k)\sigma^{k-1}(P_{k-1}) \dots \sigma(P_1)P_0$.

This sequence of prefixes is not arbitrary; it satisfies a combinatorial condition given by the prefix automaton.

Definition 2.2. The *prefix automaton* associated with a substitution σ is the automaton whose states are indexed by the letters of the alphabet $\mathcal{A}$, and whose transitions are labeled by the strict prefixes of images of letters. There is a transition from state a to state b, indexed by P, if Pa is a prefix of $\sigma(b)$.

Example 2.3. The tribonacci substitution $\breve{\sigma}$ is defined on the alphabet $\{1, 2, 3\}$ by $\breve{\sigma}(1) = 12$, $\breve{\sigma}(2) = 13$, $\breve{\sigma}(3) = 1$.

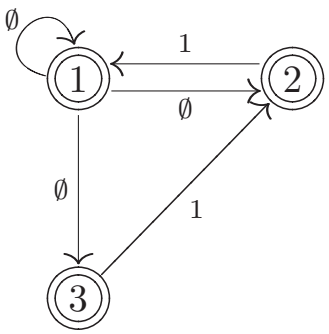

FIGURE 1. The tribonacci prefix automaton.

The only nonempty prefix is 1; the prefix automaton is shown in Figure 1, and the admissible sequences of prefixes are exactly those that do not contain three consecutive 1's.

2.3. Canonical Stepped Line Associated with a Substitution

2.3.1. Stepped Lines: Basic Definitions.

We begin with a definition.

Definition 2.4. A *stepped line* $\mathbf{L} = (x_n)_{n\geq 0}$ in $\mathbb{R}^d$ is a sequence (it could be finite or infinite) of points in $\mathbb{R}^d$ such that the *steps* $x_{n+1} - x_n$ belong to a *finite* set.

A *canonical stepped line* is a stepped line such that $x_0 = 0$ and for all $n \geq 0$, $x_{n+1} - x_n$ belongs to the canonical basis $\mathcal{B}$ of $\mathbb{R}^d$.

If $\mathcal{A}$ is a finite alphabet, there is an obvious bijection between canonical stepped lines in $\mathbb{R}^{\mathcal{A}}$ and words on the alphabet $\mathcal{A}$, which we will make explicit:

Definition 2.5. The *abelianization* map $e : \mathcal{A}^* \to \mathbb{Z}^{\mathcal{A}}$ is defined for any $W \in \mathcal{A}^*$ by $e(W) = (|W|_a)_{a\in\mathcal{A}}$, where $|W|_a$ is the number of occurrences of the letter a in W.

It will be convenient to use the notation $e_a = e(a)$ for the basis vector, and to write, for any word $W = w_1 \dots w_n$ of length n in $\mathcal{A}^*$, $e_W = e(W) = \sum_{k=1}^{n} e_{w_k}$.

Using this map, we can associate to any finite or infinite word W a canonical stepped line $\mathbf{L}^W$ in $\mathbb{R}^{\mathcal{A}}$ as the sequence (e_{P_n}), where the P_n are the prefixes of length n of W. We will sometimes refer to the (unordered) set $\mathcal{V}^W = \cup_{n\geq 0}\{x_n^W\}$ of vertices of the stepped line. We will denote by $\mathbf{L}_n^W$ (respectively $\mathcal{V}_n^W$) the finite stepped line associated with the prefix of W of length n (its set of vertices).

Remark 2.6. A canonical stepped line is a discrete set of points. There is a natural geometric curve underlying this stepped line, made up of oriented segments linking the successive vertices of the stepped line (we shall let the reader supply the formal definition). This underlying curve will appear in Section 2.5 and in Section 6.

2.3.2. Stepped Lines Associated with Substitutions: Combinatorial Properties.

We now fix a substitution σ. This paper will be concerned with a particular type of canonical stepped line:

Definition 2.7. An infinite canonical stepped line associated with a periodic point of the substitution σ is called a *canonical stepped line associated with* σ.

Recall that by definition, the abelianization map satisfies for any word $W \in \mathcal{A}^*$, the relation

$$e_{\sigma(W)} = M_\sigma e_W .$$

From this, we deduce easily a first decomposition of the prefixes of the canonical stepped lines associated with σ.

Proposition 2.8. *For any letter $a \in \mathcal{A}$, we have a disjoint decomposition*

$$\begin{aligned}\mathcal{V}^{\sigma^{n+1}(a)} &= \coprod_{P,b|Pb \text{ a prefix of } \sigma(a)} \mathcal{V}^{\sigma^n(b)} + e_{\sigma^n(P)} \\ &= \coprod_{P,b|Pb \text{ a prefix of } \sigma(a)} \mathcal{V}^{\sigma^n(b)} + M_\sigma^n e_P .\end{aligned}$$

Proof: This is a direct consequence of the trivial relation $\sigma^{n+1}(a) = \sigma^n(\sigma(a))$. □

This decomposition is valid only for finite stepped lines; a slightly more subtle decomposition, valid for infinite stepped lines, is related to the following notion:

Definition 2.9. Let $u \in \mathcal{A}^{\mathbb{N}}$. The point $x_n \in \mathbf{L}^u$ is of *type* a if $u_{n+1} = a$. We denote by $\mathcal{V}^{u,a}$ the sets of vertices of $\mathbf{L}^u$ of type a.

The fixed points of a substitution satisfy the following similarity property:

Proposition 2.10. *Let u be an infinite fixed point of the substitution σ. Then we have the disjoint decomposition*

$$\mathcal{V}^{u,a} = \coprod_{P,b|Pa \text{ a prefix of } \sigma(b)} M_\sigma \mathcal{V}^{u,b} + e_P .$$

Proof: This is a simple consequence of the fact that if x_n is of type a, then the corresponding prefix $P_{n+1} = P_n a$ of the fixed point u can be written $P_{n+1} = \sigma(P_k)Pa$, where $P_{k+1} = P_k b$ and Pa is a prefix of $\sigma(b)$. □

Remark 2.11. These relations can be viewed as examples of graph-directed iterated function systems, except for the fact that the maps involved are not contracting. Note that the graph involved in Proposition 2.8 is the opposite of the graph involved in Proposition 2.10 (the directions of the edges of the graph are reversed), and the associated adjacency matrix is transposed; these two relations are, in some sense, dual.

2.4. Stepped Lines in Contracting Spaces and Rauzy Fractals

A basic property of a canonical stepped line associated with a substitution is the following:

Proposition 2.12. *Let $E \oplus F$ be a splitting of $\mathbb{R}^{\mathcal{A}}$ that is invariant under the action of M_σ. If the restriction of M_σ to E is strictly contracting, then any canonical stepped line associated with σ stays within bounded distance of F.*

Proof: Using the prefix automaton, we can decompose any prefix of a periodic point as

$$\sigma^k(P_k)\sigma^{k-1}(P_{k-1}) \dots \sigma(P_1)P_0$$

The image of this prefix by the abelianization map is

$$\begin{aligned} e(\sigma^k(P_k)\sigma^{k-1}(P_{k-1}) \dots \sigma(P_1)P_0) &= \sum_{i=0}^{k} e(\sigma^i(P_i)) \\ &= \sum_{i=0}^{k} M_\sigma^i . e_{P_i} . \end{aligned}$$

The projection of this sum onto E is a sum whose general term decreases geometrically fast; hence this projection is bounded. □

This proposition has an immediate consequence:

Corollary 2.13. *Let $E \oplus F$ be a splitting of $\mathbb{R}^{\mathcal{A}}$ that is invariant under the action of M_σ. If the restriction of M_σ to E is strictly contracting, the projection of the vertices of the canonical line on E along F is a bounded set.*

In the case of the projection onto the contracting space associated with a substitution (and especially in the case of a substitution of Pisot type), the closure of this set is what is usually called the *Rauzy fractal* of the substitution, denoted by $\mathcal{R}$. This Rauzy fractal has remarkable properties. First of all, it is the solution of a graph-directed iterated function system (GIFS for short).

Proposition 2.14. *Let $\mathcal{R}_a$ be the closure of the projection of the vertices of type a, for all $a \in \mathcal{A}$. The sets $\mathcal{R}_a$ satisfy the relation*

$$\mathcal{R}_a = \coprod_{P,b|Pa \text{ is a prefix of } \sigma(b)} M_\sigma \mathcal{R}_b + \pi_E(e_P),$$

where π_E is the projection onto E along F.

This is an immediate consequence of Proposition 2.10. Note that since the restriction of M_σ to E is a contraction, this relation uniquely defines the $\mathcal{R}_a$ and their union $\mathcal{R}$.

We can define an additional dynamical structure on $\mathcal{R}$. There is a natural order on the vertices of a stepped line; it allows us to define a map on the set of vertices that takes any vertex to its successor. If a vertex P is of type a, the next vertex is by definition $P + e_a$. By projection, the successor function is well defined on a dense subset of $\mathcal{R}_a$; it is a translation by the projection of e_a, hence continuous, so it extends by continuity to all of $\mathcal{R}_a$. This defines, in the general case, a pseudogroup of transformations acting on the subsets $\mathcal{R}_a \subset \mathcal{R}$. If these sets are disjoint, each point is in the domain of exactly one generator of the pseudogroup, and the successor map extends to all of $\mathcal{R}$ (except perhaps on boundaries of $\mathcal{R}_a$), defining an exchange of pieces (in a number of interesting cases, the sets are disjoint up to a set of measure zero, and the map is defined except on a set of measure zero).

Example 2.15. (The original Rauzy fractal.) A classical example, which is the basis for this paper, is the tribonacci substitution $\breve{\sigma}$, first studied by Rauzy and defined above, in Example 2.3. The associated matrix has an unstable space of dimension 1 (the Perron–Frobenius expanding line) and a stable space of dimension 2, on which the action of the abelianized matrix is conjugate to the action on $\mathbb{C}$ by multiplication by μ, where μ is one of the two complex contracting eigenvalues.

Using the prefix automaton, and choosing a complex structure on the contracting plane such that $f(1)$ projects to 1 and the action of the abelianized matrix corresponds to multiplication by μ, we see that any vertex of the stepped line associated with the substitution projects onto the contracting plane to a finite sum $\sum_0^k \epsilon_i \mu^i$, where (ϵ_i) is a sequence of 0's and 1's such there are no three consecutive 1's. The closure of the projection onto the contracting plane is the Rauzy fractal (as defined above)

of the tribonacci substitution; we will call it the tribonacci fractal for short and denote it by $\breve{\mathcal{R}}$.

2.5. Stepped Lines in Expanding Spaces and Fractal Curves

Instead of projecting onto a contracting space, we can project onto an expanding space; in that case, we obtain a discrete line that tends to infinity. We will show that by renormalizing this discrete line in a suitable way, we can obtain another interesting object.

2.5.1. Projection onto the Perron–Frobenius eigenline, Tiling, and Number Systems.

Let λ be the Perron–Frobenius eigenvalue, and let $E_\lambda \oplus E_\lambda^*$ be the invariant splitting given by the Perron–Frobenius eigenline and its invariant complement. We denote by Π_λ the projection onto E_λ along E_λ^*; its restriction to the geometric curve underlying any canonical stepped line is a bijection, since E_λ^* is the orthogonal of the dual Perron–Frobenius eigenvector, which is strictly positive; hence the curve intersects each hyperplane parallel to E_λ^* exactly once.

This projection gives us a natural tiling of E_λ, which is self-similar. Is also gives us a parameterization of the canonical line, and a number system, in the following way.

Let $a \in \mathcal{A}$. The stepped line $\mathbf{L}^{\sigma^n(a)}$ projects to the interval $[0, \Pi_\lambda e_{\sigma^n(a)}] = [0, \lambda^n \Pi_\lambda e_a]$ of E_λ. It is an immediate consequence of the definition of the prefix automaton that for any vertex $x \in \mathcal{V}^{\sigma^n(a)}$, we can find a finite sequence $(P_1, \dots, P_n)$ of prefixes and a sequence $(a_0 = a, \dots, a_n)$ of letters such that $P_k a_k$ is a prefix of $\sigma(a_{k-1})$ for $k = 1, \dots, n$. The corresponding word can then be written $\sigma^{n-1}(P_1) \dots \sigma^k(P_{n-k}) \dots P_n$, and an immediate computation shows that we can write

$$\Pi_\lambda(x) = \sum_{k=1}^{n} \lambda^{n-k} \Pi_\lambda(e_{P_k}).$$

If we apply a homothety of ratio λ^{-n} to E_λ, the interval $[0, \Pi_\lambda e_{\sigma^n}(a)]$ is sent to $[0, \Pi_\lambda e_a]$, and it is not difficult to check that for any y in this interval, there is a uniquely defined sequence $(P_n)_{n\in\mathbb{N}}$ that is admissible in the sense above, and such that $y = \sum_{k=1}^{\infty} \lambda^{-k} \Pi_\lambda(e_{P_k})$; it can be viewed as an expansion in base λ, the digits being the $\Pi_\lambda(e_P)$, for all prefixes of images of letters; they form a finite set.

Remark 2.16. This construction has already been considered and studied in detail in [Dumont and Thomas 93]. There is not one number system, but a finite collection, one system for each letter. If the letter a is the beginning of an infinite word that is fixed or periodic for the substitution, this number system extends in a natural way to the positive line, but not otherwise.

Observe that the sequence of prefixes is determined by the prefix automaton, *with the arrows reversed*. A point x in the interval has a finite expansion if and only if there is $N \in \mathbb{N}$ such that $\lambda^N x$ is a vertex of the tiling obtained by projecting $\sigma^N(a)$ (this property is then true for all $n \geq N$).

2.5.2. Stepped Lines in Expanding Spaces.

Let $E \oplus F$ be an invariant splitting of $\mathbb{R}^{\mathcal{A}}$ such that the restriction of M_σ to F is strictly expanding, and denote by Π_F the projection onto F along E. We consider the projection of the stepped lines $\mathbf{L}^{\sigma^n(a)}$ onto F. It is clear that unless $\Pi_F(e_a) = 0$, these stepped lines tend to infinity, since their endpoints are $\Pi_F(e_{\sigma^n(a)}) = M_\sigma^n \Pi_F(e_a)$. We will show that after an appropriate renormalization, these stepped lines converge. We begin with an elementary fact.

Lemma 2.17. *For all $a \in \mathcal{A}$ and all $0 \leq i \leq |\sigma(a)|$,*

$$\Pi_F(x_i^{\sigma^n(a)}) = \sum_{k=1}^{n} M_\sigma^{n-k} \Pi_F(e_{P_k}),$$

where $\sigma^{n-1}(P_1) \dots \sigma(P_{n-1}) P_n$ is the prefix decomposition of the prefix of $\sigma^n(a)$ of length i *(note that this decomposition is ordered in the opposite direction compared to the previous section).*

Proof: The existence of the prefix decomposition of any prefix P of $\sigma^n(a)$, given by $P = \sigma^{n-1}(P_1) \dots \sigma(P_{n-1}) P_n$, has been shown above by the analysis of the prefix automaton. It immediately implies the formula. □

From this lemma, we easily prove the following:

Lemma 2.18. *For all $a \in \mathcal{A}$, the set*

$$\overline{\cup_{n\geq 0} M^{-n} \Pi_F(\mathcal{V}^{\sigma^n(a)})}$$

is a compact connected set.

Proof: Since

$$M\mathcal{V}^{\sigma^n(a)} \subset \mathcal{V}^{\sigma^{n+1}(a)},$$

the sets $M^{-n}\Pi_U(\mathcal{V}^{\sigma^n(a)})$ form an increasing sequence. They are uniformly bounded, by an argument similar to

the argument that proves the existence of the Rauzy fractal, the geometric series being taken in the other direction. Indeed, let $y \in M^{-n}\Pi_U(\mathcal{V}^{\sigma^n(a)})$. By the previous lemma, we can write $y = \sum_{j=1}^{n} M_\sigma^{-j}\Pi_F(e_{P_j})$. Since the e_P form a finite set, and M_σ is a strict contraction on F, this sum is uniformly bounded by a geometric series.

A similar argument shows that this set is well chained, hence connected. □

The limit set is in fact the image of a parameterized curve, which can be given explicitly. We have shown that the projection Π_λ is a bijection from the curve underlying the canonical stepped line $\mathbf{L}^{\sigma^n(a)}$ to the interval $[0, \lambda^n\Pi_\lambda(e_a)]$. We denote by γ the reciprocal map (that is, the natural parameterization of the curve by the Perron–Frobenius space).

We define a sequence of parameterized curves $\mathcal{C}_n^a : [0, \Pi_\lambda(e_a)] \to F$ by

$$\mathcal{C}_n^a(t) = M^{-n}\Pi_F(\gamma(\lambda^n t)).$$

Proposition 2.19. *The sequence of parameterized curves $\mathcal{C}_n^a$ tends uniformly to a curve $\mathcal{C}^a$, which is defined by*

$$\mathcal{C}^a(t) = \sum_{j=1}^{\infty} M_\sigma^{-j}\Pi_F(e_{P_j}),$$

where $t\Pi_\lambda(e_a) = \sum_{j=1}^{\infty} \lambda^{-j}\Pi_\lambda(e_{P_j})$ is the expansion of $t\Pi_\lambda(e_a)$ in the Dumont–Thomas number system in base λ associated with a (as in Remark 2.16).

Proof: This is a simple computation. If t has a finite expansion of degree N, all $\mathcal{C}_n^a(t)$ are equal for $n > N$, and given by the formula above; otherwise, they converge geometrically fast to it. □

We get in this way a family of curves $(\mathcal{C}^a)_{a\in\mathcal{A}}$; as we shall see later, they are quite often of Peano type, with dimension greater than 1. Their images $\mathcal{R}_a^* = \{\mathcal{C}^a(t) \mid 0 \le t \le \Pi_\lambda(e_a)\}$ satisfy an interesting relation:

Proposition 2.20. *We have*

$$\mathcal{R}_a^* = \bigcup_{P,b|Pb \text{ is a prefix of } \sigma(a)} M^{-1}(\mathcal{R}_b^* + \pi_F(e_P)).$$

Proof: The sets $M^{-n}\mathcal{V}^{\sigma^n(a)}$ are contained in $\mathcal{R}_a^*$, and their union is dense. The proposition is then an immediate consequence of Proposition 2.8. □

We observe again that we have a graph-directed IFS, which is dual to the one defined for the Rauzy fractal; the Rauzy fractal $\mathcal{R}$ and its dual $\mathcal{R}^*$ live in different spaces, and they have no reason to be similar.

2.6. Stepped Lines Associated with Interval Exchange Transformations

2.6.1. Bounded Stepped Lines in One-Dimensional Space.

There is a completely different way to build a bounded stepped line, independently of any substitution. Consider a minimal interval exchange transformation T on k intervals $I_1, \dots, I_k$ of translation length $t_1, \dots, t_k$ (that is, $T(x) = x + t_i$ if $x \in I_i$). Take any point x in the domain, and consider the itinerary with respect to the partition; we obtain an infinite word and a canonical stepped line in $\mathbb{R}^k$. Consider the projection from $\mathbb{R}^k$ to $\mathbb{R}$ that sends e_i to t_i. It is clear that the image of the canonical stepped line is bounded, the closure of its image is the domain of T, and the exchange of pieces associated with this stepped line is well defined and is the initial map T. Indeed, the image of the stepped line is, by definition, the orbit of x by T. This stepped line can be realized in $\mathbb{R}^k$ by projecting onto a one-dimensional space along the plane $\sum t_i x_i = 0$.

If the map T is self-induced on a subinterval, and if we take for x the fixed point of the map that conjugates T to the induced map, then the itinerary of x is the fixed point of a substitution.

However, it is in general difficult, for a given substitution σ, to find corresponding translation lengths t_i, to check whether the substitution dynamical system is conjugate (at least measurably) to an interval exchange transformation, and to recover the interval exchange transformation in a systematic way; we will do this below for a particular substitution.

2.6.2. Discrete Stepped Lines Associated with Algebraic Interval Exchange Transformations.

The following construction, due to [McMullen 09], associates to any algebraic interval exchange transformation a discrete curve on a slice of a lattice.

Let α be an algebraic integer of degree d, and suppose that all the lengths of the intervals, and hence all the translation lengths, belong to $\frac{1}{N}\mathbb{Z}[\alpha]$ for some N. Then the orbit of 0 is in $\frac{1}{N}\mathbb{Z}[\alpha]$, which can be considered a lattice $\mathbb{Z}^d$ by taking the vector $(n_0, \dots, n_{d-1}) \in \mathbb{Z}^d$ to $\sum_{i=0}^{d-1} \frac{n_i}{N}\alpha^i$; we define in this way a stepped line in $\mathbb{Z}^d$, which is included in a slice of $\mathbb{Z}^d$, since all points satisfy $\sum_{i=0}^{d-1} \frac{n_i}{N}\alpha^i \in I$, where I is the domain of the interval exchange transformation.

All self-similar interval exchange transformations, and in particular all interval exchange transformations related to pseudo-Anosov maps, are algebraic, and allow this construction; we will see a particular case below.

3. THE SETTING: DEFINITIONS AND NOTATION

3.1. The Interval Exchange Transformation

3.1.1. The Transformation.

For any interval $[a,b) \subset [0,1)$, we define the involution $I_{[a,b)}$ on $[0,1)$ that exchanges the two halves of the interval $[a,b)$ by a translation and fixes the complement. This involution is explicitly given by

$$I_{[a,b)} : x \mapsto \begin{cases} x + \frac{b-a}{2} & \text{if } a \le x < \frac{a+b}{2}, \\ x - \frac{b-a}{2} & \text{if } \frac{a+b}{2} \le x < b, \\ x & \text{if } x \notin [a,b). \end{cases}$$

Let α be the unique real number such that $\alpha^3 + \alpha^2 + \alpha = 1$. Define the partition $\mathcal{J} = \{J_a, J_b, J_c\} = \{[0,\alpha), [\alpha, \alpha+\alpha^2), [\alpha+\alpha^2, 1)\}$. The map T is defined as $I_{[0,1)} \circ I_{J_a} \circ I_{J_b} \circ I_{J_c}$: we cut each of the three intervals into two equal halves, exchange these halves by translation, and then rotate the circle by $\frac{1}{2}$.

The map T is an interval exchange transformation on the circle with six intervals of continuity (if we consider it as an interval exchange transformation on the interval $[0,1)$, another discontinuity is introduced by the preimage of 0, and we get an interval exchange transformation on seven intervals). The map T is conjugate to its inverse, by $T = I_{[0,1)} \circ T^{-1} \circ I_{[0,1)}$.

The map T has $\breve{\sigma}$-structure with respect to the partition $\mathcal{J}$ for the tribonacci substitution $\breve{\sigma}$ (see [Arnoux 88]). More precisely, let h be the map $h : [0,1) \to J_a = [0,\alpha)$ defined by

$$h : x \mapsto \begin{cases} \alpha x + \frac{\alpha+\alpha^4}{2} & \text{if } x < \frac{\alpha+\alpha^2}{2}, \\ \alpha x + \frac{-\alpha+\alpha^4}{2} & \text{if } x \ge \frac{\alpha+\alpha^2}{2}. \end{cases}$$

A straightforward computation proves that h conjugates T to the induced map T_{J_a}; the first-return time is 1 on $h(J_c)$, and 2 on its complement; we can check easily that $J_a = h(J_a) \cup h(J_b) \cup h(J_c)$, $J_b = T(h(J_a))$, $J_c = T(h(J_b))$.

Hence we obtain a semiconjugacy between the interval exchange transformation T and the tribonacci shift. One can prove that this semiconjugacy is a measurable conjugacy, that is, it is almost everywhere one-to-one, but it is not one-to-one everywhere, because the partition $\mathcal{J}$ is not generating; indeed, because of the discontinuity in h, $h(J_a)$ is not an interval, but the union of two disjoint intervals, and $h^2(J_a)$ has three connected components, as well as the $h^n(J_a)$ for $n > 2$.

We define the points $\alpha_1 = \frac{\alpha^4}{2} = \alpha - \frac{1}{2}$, $\alpha_2 = \alpha^2 + \frac{\alpha^4}{2} = \alpha + \alpha^2 - \frac{1}{2}$, and $\alpha_3 = \frac{1}{2}$. They cut $\mathbb{S}^1$ into the respective intervals $T(J_a)$, $T(J_b)$, and $T(J_c)$. A computation proves that $h(\alpha_1) = \alpha_2$, $h(\alpha_2) = \alpha_3$, $h(\alpha_3) = \alpha_1$, that is, $\{\alpha_1, \alpha_2, \alpha_3\}$ is a periodic orbit for h. One can prove that $\cap_{n\in\mathbb{N}} h^n(J_a)$ consists of these three points, which have the same itinerary with respect to $\mathcal{J}$ (the fixed point of σ).

3.1.2. The Partitions.

The starting point of the present paper is the partition presented in this section; it has the property that its elements are continuity intervals of the interval exchange transformation, and their images by the conjugacy are also intervals.

We would like to obtain a partition by intervals with a σ-structure. For this, we must introduce the discontinuity point of h. This in turn introduces new cutting points, and computation shows that to obtain a σ-structure with a partition by intervals, we need no fewer than nine intervals, which are bounded by the discontinuity points of the interval, plus the discontinuity point of h and its two preimages by h.

Remark 3.1. We denote the discontinuity point of h by $\beta_2 = \frac{\alpha+\alpha^2}{2}$, its preimage by $\beta_1 = \frac{\alpha^2+\alpha^4}{2}$, and its second preimage by $\beta_3 = \alpha + \frac{\alpha^2+\alpha^3}{2}$, or $\beta_0 = -\frac{\alpha^2+\alpha^3}{2} = \beta_3 \bmod 1$). These last three points are the images under T of the points $0, \alpha, \alpha^2$, and the opposites on the circle of the other discontinuity points; they are discontinuity points for the inverse map T^{-1}.

Let $\mathcal{A} = \{1, \dots, 9\}$. We consider the partition

$$\mathcal{I} = \{I_i, i \in \mathcal{A}\}$$

of the circle $\mathbb{S}^1$ into nine successive intervals (left closed, right open), with $I_1 = [0, \frac{\alpha^2+\alpha^4}{2})$ and of respective lengths

$$\frac{\alpha^2+\alpha^4}{2}, \frac{\alpha^3}{2}, \frac{\alpha^2}{2}, \frac{\alpha^3+\alpha^4}{2}, \frac{\alpha^2}{2}, \frac{\alpha^3}{2}, \frac{\alpha^4+\alpha^5}{2}, \frac{\alpha^3}{2}, \frac{\alpha^3}{2}.$$

This partition is defined by the six discontinuity points $0, \alpha/2, \alpha, \alpha+\alpha^2/2, \alpha+\alpha^2, \alpha+\alpha^2+\alpha^3/2$ of T (on the circle) and by the three points β_i (defined in Remark 3.1). It is a refinement of the natural partition by the continuity intervals; hence T can also be viewed as an interval exchange transformation on this partition.

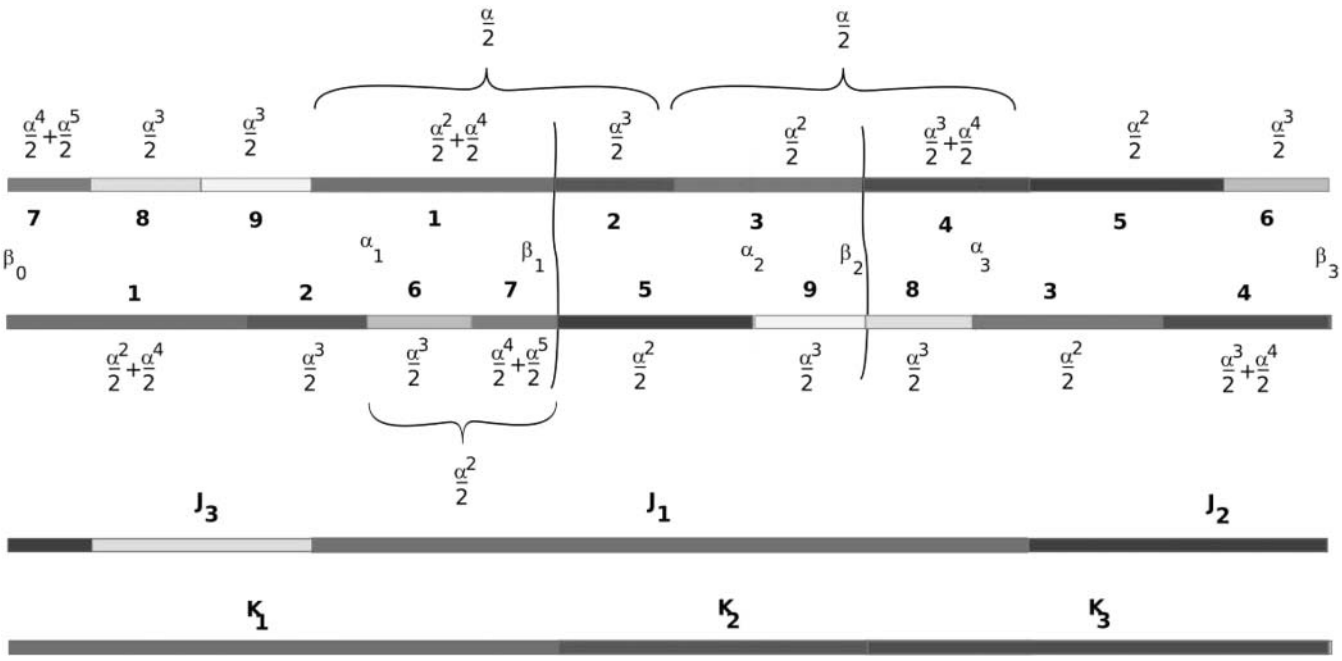

FIGURE 2. The partitions of the interval.

In what follows, it will be more convenient for computations to consider T as defined on an interval. It turns out to be inconvenient to split the circle at 0, because this introduces a new discontinuity. But the points β_n are images of discontinuity points for T; hence, if we split the circle at β_i, we get a better model. From now on, we will consider T as defined on the interval $[\beta_0, \beta_3)$. This is the convention used in Figure 2, and this is why the intervals appear in the order $(7, 8, 9, 1, 2, 3, 4, 5, 6)$, and their images in the order $(1, 2, 6, 7, 5, 9, 8, 3, 4)$. The translation vector is given by

$$t = \frac{1}{2}\big(\alpha - 1,\ \alpha - 1,\ 1 - \alpha,\ 1 - \alpha,\ \alpha^2 - 1,\ -1 - \alpha^2,\ 1 - \alpha^2,\ 2 - \alpha - \alpha^2,\ \alpha + \alpha^2\big).$$

We will denote by t_i the components of t.

The partition $\mathcal{I}$ is finer than the partition $\mathcal{J}$ defined above, since $J_a = I_1 \cup I_2 \cup I_3 \cup I_4$, $J_b = I_5 \cup I_6 \cup I_7$,$J_c = I_8 \cup I_9$. It is also finer than the partition by continuity intervals, since $I_1 \cup I_2$, $I_3 \cup I_4$, and $I_6 \cup I_7$ are continuity intervals.

We define another partition $\mathcal{K}$ by

$$\begin{aligned}\mathcal{K} &= \{K_1, K_2, K_3\}\\ &= \{I_7 \cup I_8 \cup I_9 \cup I_1, I_2 \cup I_3, I_4 \cup I_5 \cup I_6\}\\ &= \{T(I_1) \cup T(I_2) \cup T(I_6) \cup T(I_7), T(I_5) \cup T(I_9),\\ &\quad T(I_8) \cup T(I_3) \cup T(I_4)\},\end{aligned}$$

so that $K_1 = [\beta_0, \beta_1)$, $K_2 = [\beta_1, \beta_2)$, and $K_3 = [\beta_2, \beta_3)$. The lengths of these intervals are $|K_1| = \frac{\alpha+\alpha^2}{2}$ (contains the origin), $|K_2| = \frac{\alpha^2+\alpha^3}{2}$, and $|K_3| = \frac{\alpha+\alpha^3}{2}$. As we will see below, this partition plays an important role in the induction.

Definition 3.2. We denote by k^- and k^+ the two maps from the alphabet $\mathcal{A}$ to $\{1, 2, 3\}$ defined by $I_i \subset K_{k^-(i)}$ and $T(I_i) \subset K_{k^+(i)}$.

Finally, we consider the partition $\hat{\mathcal{J}} = \mathcal{J} \vee \mathcal{K}$:

$$\begin{aligned}\hat{\mathcal{J}} &= \{\hat{J}_1, \hat{J}_2, \hat{J}_4, \hat{J}_5, \hat{J}_7, \hat{J}_9\}\\ &= \{I_1, I_2 \cup I_3, I_4, I_5 \cup I_6, I_7, I_8 \cup I_9\},\end{aligned}$$

which is indexed by the alphabet $\hat{\mathcal{A}} = \{1, 2, 4, 5, 7, 8\} \subset \mathcal{A}$. This partition will arise naturally in the geometric constructions of Sections 6.1 and 6.2.

3.1.3. The McMullen Curve.

The map T is algebraic; hence it allows the construction explained in Section 2.6.2. This construction will be detailed in Section 6.3. For now, observe that all lengths of the intervals of T belong to $\frac{1}{2}\mathbb{Z}[\alpha]$. We can map $\mathbb{Z}^3$ bijectively onto $\frac{1}{2}\mathbb{Z}[\alpha]$ by the map

$$Q : (n, p, q) \mapsto \frac{n}{2} + \frac{p}{2}\alpha + \frac{q}{2}\alpha^2.$$

We observe that $\mathcal{Z} = Q^{-1}(\frac{1}{2}\mathbb{Z}[\alpha] \cap [\beta_0, \beta_3))$ is a "slice" in $\mathbb{Z}^3$ between two planes. Note that for all $(p, q) \in \mathbb{Z}^2$, there is a unique n such that $Q(n, p, q) \in [\beta_0, \beta_3)$, $Q(n+1, p, q) \in [\beta_0, \beta_3)$, i.e., there are exactly two points of type (n, p, q) for a fixed pair (p, q) in the slice (the original curve was defined using the interval $[0, 1)$ instead of $[\beta_0, \beta_3)$, but this would be less convenient).

We will call the curve underlying the stepped line (denoted by $\mathcal{L}$) between successive points $(Q^{-1}(T^n(\alpha_1)))_{n\geq 0}$ of the orbit of the fixed point seen in $\mathbb{Z}^3$ the *McMullen curve*; see the figure in [McMullen 09]. It is a stepped line, since the differences $Q^{-1}(T^{n+1}(\alpha_1)) - Q^{-1}(T^n(\alpha_1))$ are given by the $Q^{-1}(t_i)$, so they assume only a finite number of values.

3.2. The Substitution

3.2.1. Definition.

We introduce the substitution σ on the alphabet $\mathcal{A}$:

$$\begin{aligned}\sigma : 1 &\to 35\\ 2 &\to 45\\ 3 &\to 46\\ 4 &\to 17\\ 5 &\to 18\\ 6 &\to 19\\ 7 &\to 29\\ 8 &\to 2\\ 9 &\to 3.\end{aligned}$$

The substitution σ has a periodic orbit of period 3. Set $u = u^{(1)} = \lim_{n\to\infty} \sigma^{3n}(1)$, $u^{(2)} = \lim_{n\to\infty} \sigma^{3n}(3)$, and $u^{(3)} = \lim_{n\to\infty} \sigma^{3n}(4)$; the periodic orbit is $u^{(1)} \xrightarrow{\sigma} u^{(2)} \xrightarrow{\sigma} u^{(3)} \xrightarrow{\sigma} u^{(1)}$. It has no other periodic orbit.

3.2.2. Dynamics

We have the following proposition:

Proposition 3.3. *The dynamical system $(\mathbb{S}^1, T)$ has a σ-structure with respect to the partition $\mathcal{I}$.*

Proof: This expresses the induction scheme. We know that the map T is conjugate by h to its induced map on $J_1 = I_1 \cup I_2 \cup I_3 \cup I_4$. We have to check the σ-structure. But a simple computation shows that $h(I_1) \subset I_3$, $T(h(I_1)) \subset I_5$, and $T^2(h(I_1)) \subset J_1$; hence the itinerary of the interval $h(I_1)$ is 35; similar computations for the other intervals show that we have a σ-structure for the substitution σ above. □

Since the elements of the partition $\mathcal{I}$ are continuity intervals for the minimal map T, the partition is generating, that is, the map $\varphi_{\mathcal{I}}$ that sends each point to its itinerary with respect to the partition $\mathcal{I}$ is one-to-one. And since we have a σ-structure, the coding of the IET T is well described by the substitutive dynamical system (Ω, S), where S denotes the usual shift, and the following diagram commutes:

$$\begin{array}{ccc}\mathbb{S}^1 & \xrightarrow{T} & \mathbb{S}^1\\ \downarrow \varphi_{\mathcal{I}} & & \downarrow \varphi_{\mathcal{I}}\\ \Omega & \xrightarrow{S} & \Omega\end{array}$$

Similarly, the following diagram, which expresses the induction, commutes:

$$\begin{array}{ccc}\mathbb{S}^1 & \xrightarrow{h} & \mathbb{S}^1\\ \downarrow \varphi_{\mathcal{I}} & & \downarrow \varphi_{\mathcal{I}}\\ \Omega & \xrightarrow{\sigma} & \Omega\end{array}$$

Remark 3.4. It is interesting, the better to see the induction, to define the interval exchange transformation on the disjoint union of the three intervals K_1, K_2, and K_3, as suggested by Figure 3.

Indeed, we can check that the conjugacy map h defined above satisfies $h(K_1) = K_2$, $h(K_2) = I_4 \subset K_3$, and $h(K_3) = I_1 \subset K_1$.

We can take local coordinates on each K_i by taking the distance to the periodic point α_i; more precisely, we define a map $[\beta_0, \beta_3) \to \mathbb{R} \times \mathbb{Z}/3\mathbb{Z}$, $t \mapsto (t - \alpha_i, i)$, if $x \in K_i$. A direct computation shows that in these coordinates, h can be written $h(x, i) = (\alpha x, i + 1)$; the cube

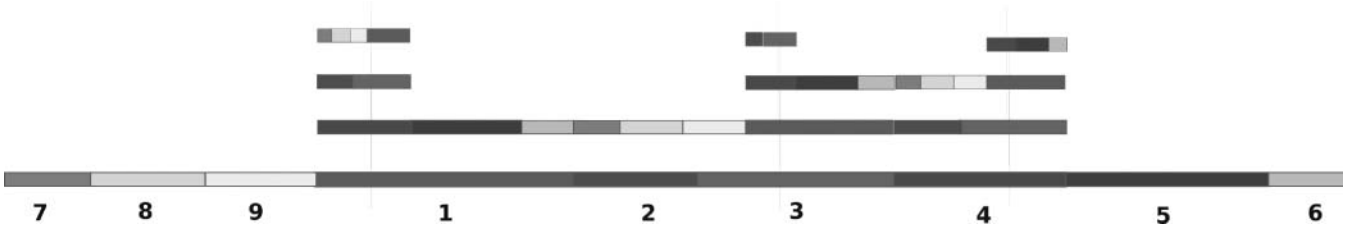

FIGURE 3. The induction.

h^3 of h is a homothety on each interval K_i, centered in α_i, as can be seen in Figure 3.

Observe that the periodic orbit of h corresponds to the periodic orbit of σ in the following way:

$$\varphi_{\mathcal{I}}(\alpha_1) = u, \quad \varphi_{\mathcal{I}}(\alpha_2) = u^{(2)}, \quad \varphi_{\mathcal{I}}(\alpha_3) = u^{(3)}. \quad (3\text{–}1)$$

We will see that this periodic structure of order 3 of the induction appears in the spectral theory for the substitution σ.

3.2.3. Factors.

There are two natural factors of this symbolic dynamical system.

The first one follows from the identification $\rho : \mathcal{A} \to \breve{\mathcal{A}} = \{a, b, c\}$ defined by $I_i \subset J_{\rho(i)}$, i.e., $1, 2, 3, 4 \mapsto a$; $5, 6, 7 \mapsto b$; $8, 9 \mapsto c$. The map ρ defines an equivalence relation on the alphabet, which extends to the free monoid $\mathcal{A}^*$: two words are equivalent if they have the same image under ρ. One checks immediately that this equivalence relation is compatible with the substitution σ, and the factor substitution is the tribonacci substitution defined above in Example 2.3:

$$\begin{aligned} \breve{\sigma} : a &\to ab \\ b &\to ac \\ c &\to a. \end{aligned}$$

The other one follows from the identification $2 \cong 3$, $5 \cong 6$, and $8 \cong 9$ and corresponds to the coding by the partition $\hat{\mathcal{J}}$. This equivalence relation is also compatible with the substitution, and the factor substitution on the alphabet $\hat{\mathcal{A}} = \{1, 2, 4, 5, 7, 8\}$ is

$$\begin{aligned} \hat{\sigma} : 1 &\to 25 \\ 2 &\to 45 \\ 4 &\to 17 \\ 5 &\to 18 \\ 7 &\to 28 \\ 8 &\to 2. \end{aligned}$$

Observe that the equivalence relation corresponding to coding by partition $\mathcal{K}$ is incompatible with σ: letters 1 and 9 are equivalent for this partition, and their images do not even have the same length; hence there is no factor substitution for this partition.

3.2.4. Linear Algebra.

The matrix M_σ associated with σ is a 9×9 matrix, whose characteristic polynomial is $P(X) = X^9 - X^7 - 5X^6 - X^5 + X^4 + 5X^3 + X^2 - 1$, which factors as

$$\begin{aligned} P(X) = (X-1)(X^2+X+1)(X^3+X^2+X-1) \\ \times (X^3 - X^2 - X - 1). \end{aligned}$$

The Perron–Frobenius eigenvalue is $\lambda = 1.8393\ldots$, the real root of $X^3 - X^2 - X - 1$. We decompose the space $\mathbb{R}^{\mathcal{A}}$ into three invariant subspaces of dimension three with rational equation corresponding to this factorization, $\mathbb{R}^{\mathcal{A}} = E_n \oplus E_T \oplus E_{\overline{T}}$, where:

- The invariant subspace E_n is associated with the eigenvalues $1, j, j^2$; it splits into $E_n = E_I \oplus E_j$, where E_I is the eigenspace associated with eigenvalue 1, and E_j is the invariant plane associated with the pair of eigenvalues j, j^2.
- The invariant subspace $E_{\overline{T}} = \ker(M^3 + M^2 + M - \mathrm{Id})$, corresponds to eigenvalues $\alpha < 1$, β, and $\overline{\beta}$, roots of $X^3 + X^2 + X - 1$, and splits into $E_{\overline{T}} = E_{\overline{T},s} \oplus E_{\overline{T},u}$, a contracting direction and an expanding plane.
- The invariant subspace $E_T = \ker(M^3 - M^2 - M - \mathrm{Id})$ corresponds to eigenvalues $\lambda > 1$, μ, and $\overline{\mu}$, and also splits into $E_T = E_{T,u} \oplus E_{T,s}$, the Perron–Frobenius direction and the contracting plane.

The space $E_{\overline{T},u} \oplus E_{T,u}$ is the invariant unstable space E_u, and the space $E_{\overline{T},s} \oplus E_{T,s}$ is the invariant stable space E_s. We summarize:

$$\begin{aligned} \mathbb{R}^{\mathcal{A}} &= E_n \oplus E_{\overline{T}} \oplus E_T = E_n \oplus E_s \oplus E_u \\ &= E_I \oplus E_j \oplus E_{\overline{T},s} \oplus E_{\overline{T},u} \oplus E_{T,u} \oplus E_{T,s}. \end{aligned} \quad (3\text{–}2)$$

If

$$A = \begin{pmatrix} 1 & 1 & 1 \\ 1 & 0 & 0 \\ 0 & 1 & 0 \end{pmatrix}$$

denotes the tribonacci matrix, and

$$J = \begin{pmatrix} 0 & 0 & 1 \\ 1 & 0 & 0 \\ 0 & 1 & 0 \end{pmatrix}$$

the permutation matrix, then the factorization of the characteristic polynomial implies that we can find a rational matrix P such that the conjugate matrix $\widetilde{M}$ is

given by

$$\widetilde{M} = P^{-1}MP = \begin{pmatrix} J & 0 & 0 \\ 0 & {}^tA^{-1} & 0 \\ 0 & 0 & A \end{pmatrix}.$$

We denote by Π_* the projection onto E_* parallel to the supplementary space according to decomposition (3–2), where E_* is any invariant subspace. This defines a family of projections $\Pi_n, \Pi_T, \Pi_{T,s}, \ldots$, and we will mostly consider these projections (except in some particular cases, where we will make explicit our choice of projection) and use them to define stepped lines.

4. THE STABLE SUBSPACE

In this section, we concentrate on what happens in the stable subspace E_s. In stable directions, the Rauzy fractal construction procedure is natural. We will see that it works well if we restrict to the two-dimensional space $E_{T,s}$ but that the situation is more intricate in the direction $E_{\overline{T},s}$. To obtain a nicer picture, we will involve the neutral direction, and recover in a systematic way the interval exchange transformation from the substitution, and a Peano curve.

4.1. Projection to the Tribonacci Stable Plane

The equivalence relation defined on $\mathcal{A}$ by the partition $\mathcal{J}$ defines a subspace of dimension 6. A small computation shows that this space is $E_n \oplus E_{\overline{T}}$; the projection Π_T onto the space E_T satisfies by construction $\Pi_T(e_1) = \Pi_T(e_2) = \Pi_T(e_3) = \Pi_T(e_4)$, $\Pi_T(e_5) = \Pi_T(e_6) = \Pi_T(e_7)$, $\Pi_T(e_8) = \Pi_T(e_9)$. If we define $e_a = \Pi_T(e_1)$, $e_b = \Pi_T(e_5)$, $e_c = \Pi_T(e_8)$, we obtain a basis of the 3-dimensional space E_T, which can be viewed as $\mathbb{R}^{\breve{\mathcal{A}}}$, on which the restriction of M acts as A.

The canonical stepped line $\mathbf{L}^{\breve{u}}$ associated with the tribonacci substitution can be embedded in this way in E_T, and we have the following result, which is not surprising in view of [Arnoux 88]:

Theorem 4.1

$$\Pi_T(\boldsymbol{L}^{u^{(i)}}) = \boldsymbol{L}^{\breve{u}} \text{ for } i = 1, 2, 3.$$

Proof: This result is a straightforward consequence of the analysis done in the previous section. Indeed, the projection ρ from $\mathcal{A}$ to $\breve{\mathcal{A}}$ sends the three periodic points $u^{(i)}$ of σ to the fixed point $\breve{u}$ of $\breve{\sigma}$, so the corresponding projection Π_T sends the three corresponding canonical stepped lines to the canonical stepped line $\mathbf{L}^{\breve{u}}$ in $E_T = \mathbb{R}^{\breve{\mathcal{A}}}$. □

As an immediate consequence, we have the following corollary:

Corollary 4.2.

$$\overline{\Pi_{T,s}(\mathcal{V}^u)} = \breve{\mathcal{R}}.$$

The vertices of the stepped line project onto the tribonacci fractal. The partition $\{\Pi_{T,s}(\mathcal{V}^{u,a}),\ a \in \mathcal{A}\}$ (up to sets of measure zero) is shown in Figure 4 before and after the exchange of pieces. The standard partition of the tribonacci fractal is obtained by taking the unions of tiles with the same ρ.

Remark 4.3. Observe that the same result holds for the stepped lines associated with the other fixed points, since these fixed points also project onto $\breve{u}$. This may seem paradoxical at first glance, since naturally, the three fixed points are different, though they yield the same partition. An explanation could be that the partition is up to a set of measure zero: indeed, the sets $\Pi_{T,s}(\mathcal{V}^{u^{(1)},a})$ and $\Pi_{T,s}(\mathcal{V}^{u^{(2)},a})$ differ on their boundaries, while the set of indices on which the corresponding fixed points are distinct can be of zero density.

4.2. Projection to the Stable Direction in Antitribonacci

A straightforward application of the results of Section 2.4 shows that the sets $\Pi_{\overline{T}}(\mathcal{V}^{u,a})$ are compact sets in $E_{\overline{T},s}$. They satisfy a GIFS, which can be written explicitly, using the fact that with notation introduced in Section 3.1.2, $\Pi_{\overline{T},s}(e_i) = t_i - (\alpha_{k^+(i)} - \alpha_{k^-(i)})$.

This GIFS can be solved explicitly, and the result is slightly messy: the adherences of the $\Pi_{\overline{T}}(\mathcal{V}^{u,a})$ are overlapping intervals. More precisely, we get copies of the intervals K_1, K_2, K_3, each centered at α_i, since these points correspond to the three periodic points and project to 0; hence they overlap.

We will not go into further details, since a clearer picture will emerge in the following sections.

4.3. Projection onto the Complete Stable Space

We can gather the results of the two previous subsections by considering the projection Π_s onto the space E_s parallel to $E_u \oplus E_n$. We are interested in $\Pi_s(\mathbf{L}^u)$. For the same reasons as in Section 4.2, the picture is still a little bit messy. But here, there is no overlap because the component $E_{T,s}$ separates points that would have the same projection onto $E_{\overline{T},s}$. Indeed, the projection is the union of three continuous (fractal) curves, as shown in Figure 5.

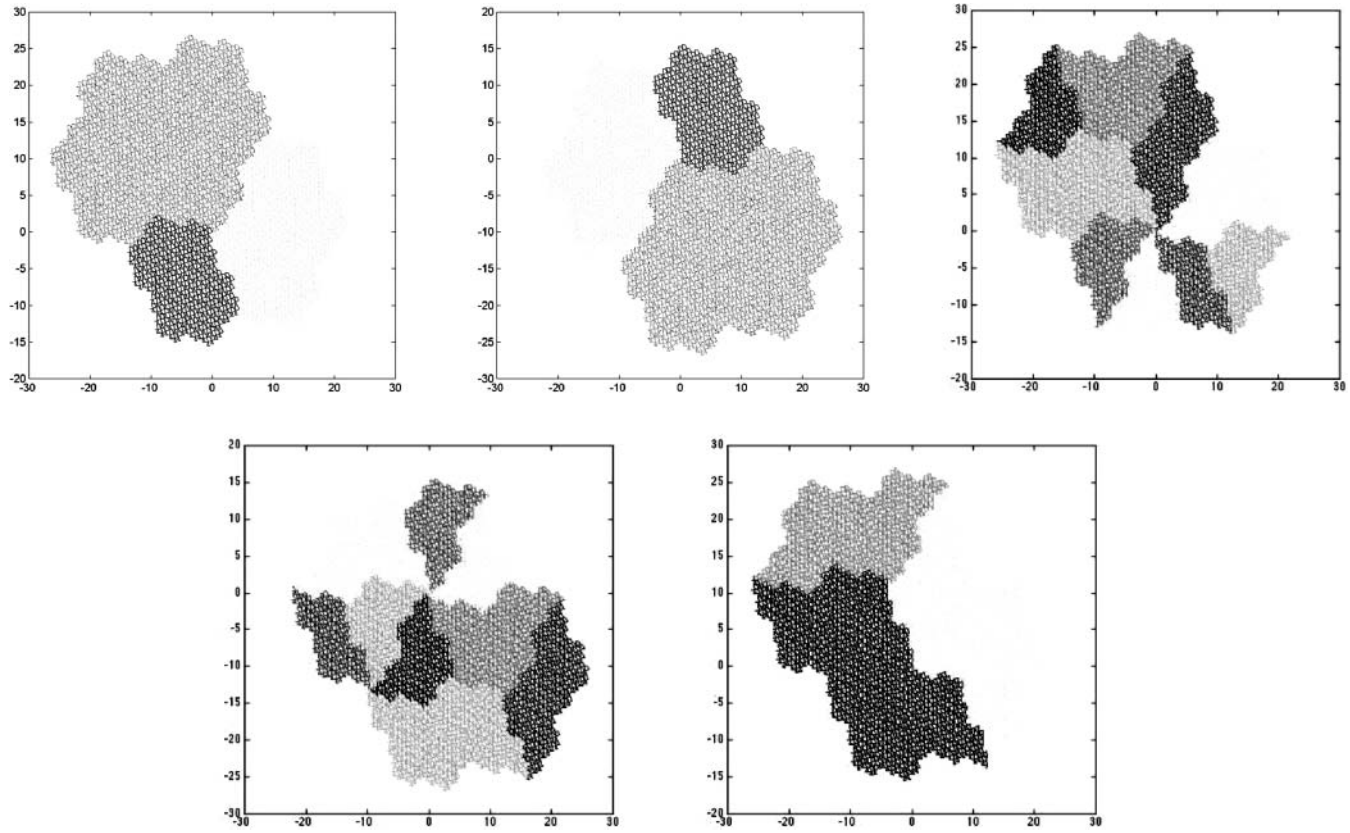

FIGURE 4. The tribonacci fractal. Partition $\mathcal{J}$ (standard tribonacci) before and after exchange, partition $\mathcal{I}$ before and after exchange, and partition $\mathcal{K}$.

Proof of such a statement would follow from Theorem 4.5, which makes explicit the complete picture.

4.4. Recovering the IET: A First Attempt Using Another Projection to $E_{\overline{T},s}$

We use the results of Section 2.6, and consider the projection $\Pi_/$ onto $E_{\overline{T},s}$ parallel to the hyperplane H of equation $\sum_{i=1}^{d} t_i x_i = 0$.

We observe that the subspace H is related to the eigenspaces as follows: $E_T \subset H$, $E_{\overline{T},u} \subset H$, $E_I \subset H$, and $H \oplus E_{\overline{T},s} = \mathbb{R}^{\mathcal{A}}$; the relation between H and E_j will appear later.

We are interested in the projection of $\mathcal{V}^u$. The following theorem is an immediate consequence of the result of Section 2.6, since the projections of the basis vectors are the translation lengths of the interval exchange transformation T.

Theorem 4.4. *$\overline{\Pi_/(\mathcal{V}^u)}$ is an interval. The subsets $\overline{\Pi_/(\mathcal{V}^{u,a})}$ are intervals with disjoint interiors, and the exchange of pieces is homothetic to the original map T.*

As we will see below, what we did by changing the projection was just to make a constant translation on each copy of the K_i to remove the overlap.

4.5. The Tribonacci Filling Curve

We want to extend the projection $\Pi_/$ to all of E_s. Recalling $E_{T,s} \subset H$, we define the projection $\Pi_{\tilde{s}}$ onto the space E_s parallel to $\tilde{H} = H \cap (E_u \oplus E_n \oplus E_{\overline{T},s})$. We can write $\Pi_{\tilde{s}} = \Pi_{T,s} \oplus \Pi_/$. We are interested in $\Pi_{\tilde{s}}(\mathcal{V}^u)$. This object lies in $E_s = E_{T,s} \oplus E_{\overline{T},s}$, which we can view as $\mathbb{R}^3$.

Theorem 4.5. *$\overline{\Pi_{\tilde{s}}(\mathcal{V}^u)}$ is a continuous curve in $\mathbb{R}^3$. Its projection onto $E_{T,s}$ parallel to $E_{\overline{T},s}$ is a Peano curve filling the tribonacci fractal $\breve{\mathcal{R}}$. Its projection onto $E_{\overline{T},s}$ parallel to $E_{T,s}$ is one-to-one, and its image is an interval.*

In other words, $\overline{\Pi_{\tilde{s}}(\mathcal{V}^u)}$ is the graph of a Peano curve filling the tribonacci fractal $\breve{\mathcal{R}}$ parameterized by the coordinate along $E_{\overline{T},s}$.

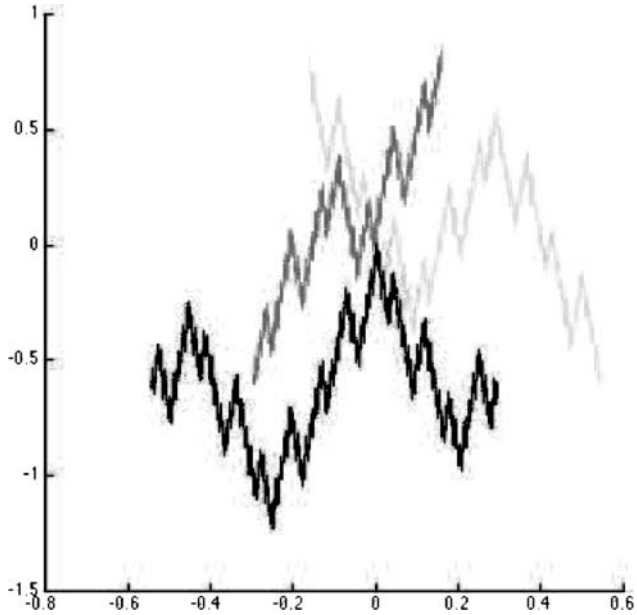

FIGURE 5. A view of $\Pi_s(\mathcal{V}^u)$. The gray levels correspond to the partition $\mathcal{K}$. Note that this is a two-dimensional view of a 3-dimensional curve with high Hausdorff dimension; this picture is to be compared with Figures 6 and 7.

Proof: Basically, this is a consequence of Theorems 4.1 and 4.4. Continuity follows from the fact that if two points are close in the direction $E_{\overline{T},s}$, they are (except for a finite number of orbits) close symbolically and hence close in E_T. More specifically, if $\Pi_/(x_n^u)$ is a point that does not belong to the orbits of boundary points of the intervals I_i, for any $N > 0$ there is a neighborhood V of $\Pi_/(x_n^u)$ such that all points in V have the same dynamics for N steps, so that any other x_m^u with $\Pi_/(x_m^u) \in V$ will satisfy $\Pi_{T,s}(x_m^u)$ close to $\Pi_{T,s}(x_n^u)$. So all we have to check is continuity at the boundaries of the atoms of the partition $\mathcal{I}$. Since it projects onto E_T, the only delicate points are the boundaries of J_a, J_b, and J_c. But they all project onto the same point. □

Observe that the points corresponding to the prefixes of the fixed point appear on the curve in an order prescribed by the dynamics, which is in a sense dual to the order in which they are disposed on the $E_{\overline{T},s}$-axis. It is a straightforward way to see the Peano curve in the tribonacci fractal constructed in [Arnoux 88] (the proof in that paper is essentially the one we just gave; the essential step is to prove that discontinuity points have the same image). Indeed, it defines a map from the interval (or the circle $\mathbb{S}^1$) to the tribonacci fractal. Observe that the sets $\overline{\Pi_{\tilde{s}}(\mathcal{V}^{u,a})}$ project onto compact disjoint (up to boundary points) pieces of the tribonacci fractal.

The fact that the projection of the stepped line is a curve is far from obvious from the construction, since we just project a discrete set in $\mathbb{R}^{\mathcal{A}}$. We will see later another way to construct this Peano curve as a limit of a sequence of renormalized stepped lines, associated with the so-called dual substitution, which gives a curve by construction.

5. THE NEUTRAL SUBSPACE

We now study in a more detailed way the dynamical behavior in the neutral subspace E_n. In general, the projections onto the neutral space can be quite complicated, since we cannot expect convergent series and there can be an unbounded drift. However, in our case, some remarkable coincidences occur, and things are quite simple and almost completely understood. Indeed, the space E_n splits into $E_j \oplus E_I$. In E_j, the Rauzy fractal procedure yields a finite set. Along E_I, the stepped line projects onto a discrete but unbounded set. We use this result to give another formulation of Theorem 4.4, making clearer the role of the partition $\mathcal{K}$.

5.1. Projection to the Neutral Subspace

We first analyze the projection of $\mathbf{L}^u$ onto the space E_j. Let $M_1 = 0$, $M_2 = -\Pi_j(e_2)$, $M_3 = \Pi_j(e_8)$, and set $\mathcal{M} = \{M_1, M_2, M_3\}$.

Theorem 5.1. *The projection of $\mathcal{V}^u$ onto E_j is reduced to $\mathcal{M}$.*

Proof: Computation (see Section 9) shows that $\Pi_j(e_1) = \Pi_j(e_4) = \Pi_j(e_7) = 0$, that $\Pi_j(e_2) = -\Pi_j(e_9)$, $\Pi_j(e_3) = -\Pi_j(e_5)$, $\Pi_j(e_6) = -\Pi_j(e_8)$, and that $\Pi_j(e_2 + e_8 + e_5) = 0$.

Consider the graph G (see Figure 8) with vertices $\{1, 2, 3\}$ and for which there is an edge from r to s labeled $(a, \Pi_j(e_a))$ if and only if $k^-(a) = r$ and $k^+(a) = s$ (where k^- and k^+ have been defined in Definition 3.2). Observe that for any $a \in \mathcal{A}$, there is exactly one edge labeled by $(a, \Pi_j(e_a))$. Any itinerary $\varphi_{\mathcal{I}}(x) = (v_n)_{n\in\mathbb{N}}$ is the label of a path in this graph, since by definition, we must have $k^-(v_{n+1}) = k^+(v_n)$; the corresponding sequence of vertices is just the itinerary $\varphi_{\mathcal{K}}(x)$ of x with respect to the partition $\mathcal{K}$.

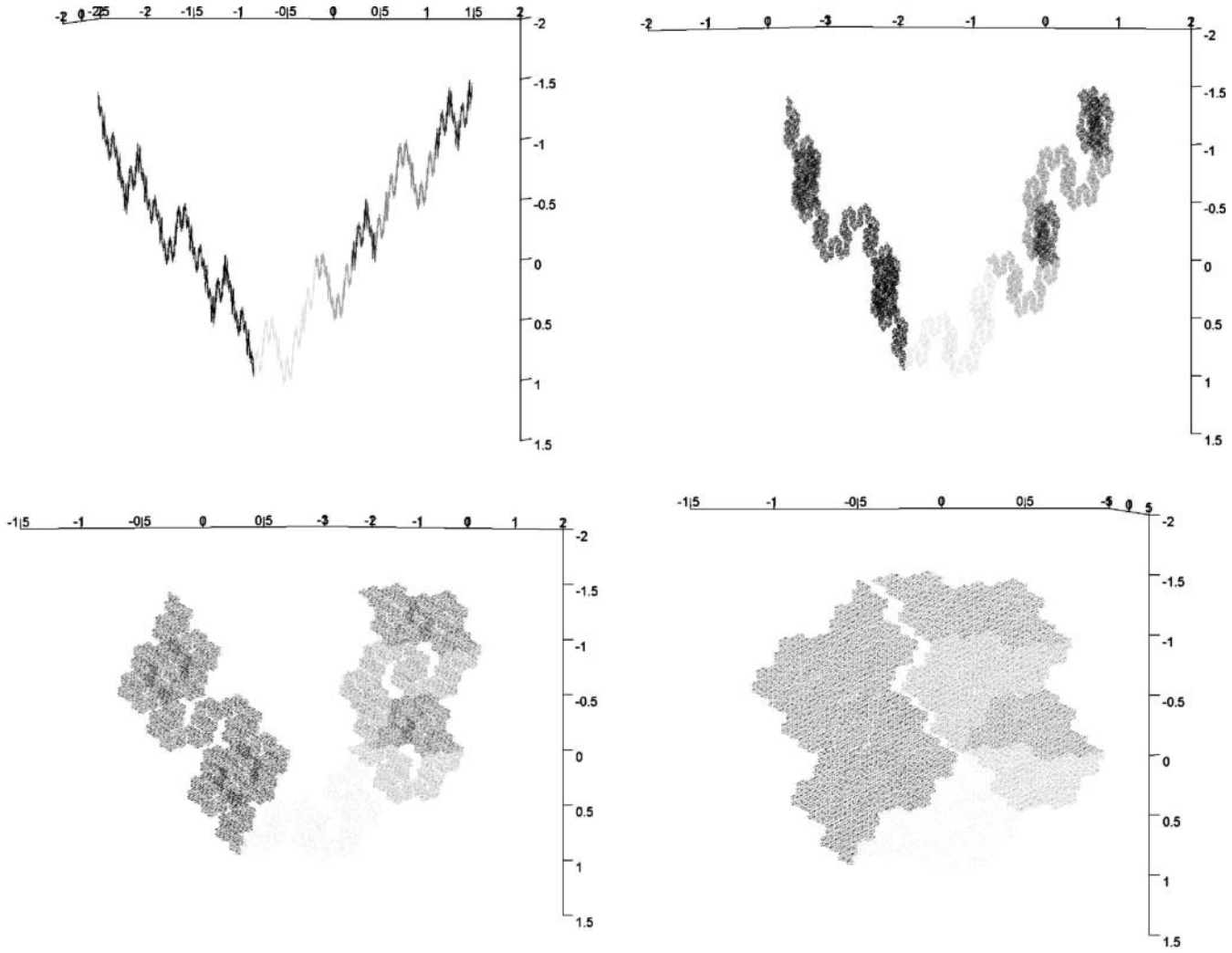

FIGURE 6. Different views of the tribonacci filling curve $\Pi_{\tilde{s}}(L^u)$. The gray levels should help in visualizing the third dimension.

This is true in particular for the fixed point u; moreover, since $u_0 = 1$, we have $I_{u_0} \subset K_1$, and the corresponding path starts from vertex 1.

One checks immediately that for all $a \in \mathcal{A}$, $\Pi_j(e_a) = M_{k^+(a)} - M_{k^-(a)}$; hence the cocycle is a coboundary, and we have, for any itinerary v,

$$\sum_{j=0}^{n} \Pi_j(e_{v_j}) = M_{k^+(v_n)} - M_{k^-(v_0)},$$

in particular, for the fixed point, $M_{k^-(v_0)} = 0$, so the projection of the corresponding canonical stepped line $\Pi_j(x_n^u)$ is in $\mathcal{M}$ for all $n \geq 1$, which proves the theorem. □

The projection to the whole space E_n is slightly more complicated. For convenience, we denote by V_1 (respectively V_2, V_3) the vector $\Pi_j(e_2)$ (respectively $\Pi_j(e_5, \Pi_j(e_8))$, and by $\Delta = -e_1 + e_3 - e_5 + e_6 - e_8 + e_9$ the invariant vector (eigenvector for the eigenvalue 1.)

Proposition 5.2. *The projection of $\mathcal{V}^u$ onto E_n is a discrete but unbounded subset of $\mathcal{M} + \mathbb{Z}\Delta/3$, namely*

$$\Pi_n(\mathcal{V}^u) = (M_1 + \mathbb{Z}\Delta) \cup (M_2 + \Delta/3 + \mathbb{Z}\Delta) \cup (M_2 + 2\Delta/3 + \mathbb{Z}\Delta).$$

Remark 5.3. It is possible to prove that the drift in the Δ-direction is logarithmic. We have no geometric interpretation for what happens in this direction.

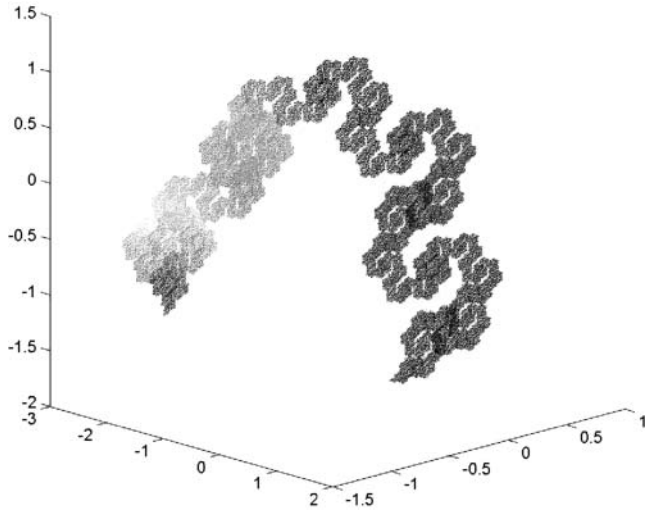

FIGURE 7. A view of the tribonacci filling curve $\Pi_{\tilde{s}}(L^u)$. Here the gray level changes continuously along the coordinate $E_{\overline{T},s}$.

Proof: Computation shows that $\Pi_n(e_2+e_8+e_5) = \Delta$ and $\Pi_n(e_3+e_6+e_9) = -\Delta$. Using the notation V_1, V_2, V_3 above, we compute the projections of the basis vectors on E_n:

$$\begin{aligned}
&\Pi_n(e_1) = \Pi_n(e_4) = \Pi_n(e_7) = 0,\\
&\Pi_n(e_2) = V_1 + \frac{\Delta}{3} = -\Pi_n(e_9),\\
&\Pi_n(e_5) = V_2 + \frac{\Delta}{3} = -\Pi_n(e_3),\\
&\Pi_n(e_8) = V_3 + \frac{\Delta}{3} = -\Pi_n(e_6).
\end{aligned}$$

Taking into account the Δ-component, we immediately see that $\Pi_n(L_n^u) \subset \mathcal{M} + \mathbb{Z}\Delta/3$. Let us first prove that the stepped line is unbounded in this direction. To do so we exhibit two sequences $W_n^{\pm}$ of prefixes of the fixed point u for which $\Pi_n(e_{W_n^{\pm}}) = \pm n\Delta/2$. Indeed, consider $W_1^- = \sigma^5(3)\sigma^3(3)\sigma(3)$ and set for all $n \geq 1$, $W_{n+1}^- = \sigma^6(W_n^-)W_1^-$. It follows from a straightforward analysis of the prefix automaton that W_n^- are prefixes of the fixed point u. Since $\Pi_n(M^3 e_i) = \Pi_n(e_i)$, it follows that

$$\begin{aligned}
\Pi_n(e_{W_n^-}) &= \Pi_n\Big(\sum_{i=1}^{n} M^{6n} e_{W_1^-}\Big) = \sum_{i=1}^{n} \Pi_n\big(M^{6n} e_{W_1^-}\big)\\
&= n\Pi_n(e_{W_1^-}).
\end{aligned}$$

Recalling that $W_1^- = \sigma^5(3)\sigma^3(3)\sigma(3)$, we conclude that

$$\begin{aligned}
\Pi_n(e_{W_n^-}) &= n\Pi_n\big(M^5 e_3 + M^3 e_3 + M e_3\big)\\
&= n\Pi_n\big(e_9 + e_3 + e_6\big) = -n\Delta.
\end{aligned}$$

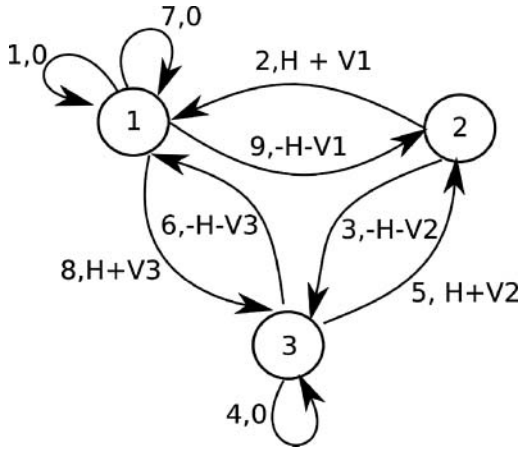

FIGURE 8. Graph of the approximating subshift: vertices are 1, 2, and 3, and edges are labeled $\mathcal{A}$ and $\{\Pi_j(e_a),\ a \in \mathcal{A}\}$, with $H = \Delta/3$.

In the same spirit, we consider

$$W_0^+ = \sigma^3(1)\sigma^2(2), \quad W_1^+ = \sigma^8(W_0^+)\sigma^4(W_0^+)W_0^+,$$

and set

$$\begin{aligned}
W_{n+1}^+ = \sigma^{12n+6}(W_0^+)\sigma^{12n}(W_1^+)\sigma^{12(n-1)}(W_1^+)\\
\cdots\sigma^{12}(W_1^+)W_1^+.
\end{aligned}$$

Again, W_n^+ is a prefix of u, and here,

$$\Pi_n(e_{W_n^+}) = n\Delta.$$

To conclude we observe that in view of the graph G, only points of the form $M_i + i\Delta/3 + n\Delta$ can be attained, since moves in direction Δ correspond to period-3 cycles in the graph. The same analysis shows that all such points are attained, since $n\Delta$ are attained for all $n \in \mathbb{Z}$. □

5.2. Recovering the IET on Three Intervals: A More Conceptual Version

Here we project the stepped line L^u onto $E_j \oplus E_{T,s}$. The Rauzy fractal we obtain is the union of three intervals that can be viewed as the three intervals K_1, K_2, and K_3 of the partition $\mathcal{K}$. We recover Lemma 4.4 by projecting in a direction such that the three intervals glue onto a single segment. We denote by $\Pi_{///}$ the natural projection onto $E_j \oplus E_{\overline{T},s}$.

Consider the set comprising the union of three intervals, copies of K_1, K_2, K_3 parallel to $E_{\overline{T},s}$, defined by

$$\begin{aligned}
\widehat{K} = (M_1 + (K_1 - \alpha_1)e^{\overline{T},s}) \cup (M_2 + (K_2 - \alpha_2)e^{\overline{T},s})\\
\cup (M_3 + (K_3 - \alpha_3)e^{\overline{T},s}).
\end{aligned}$$

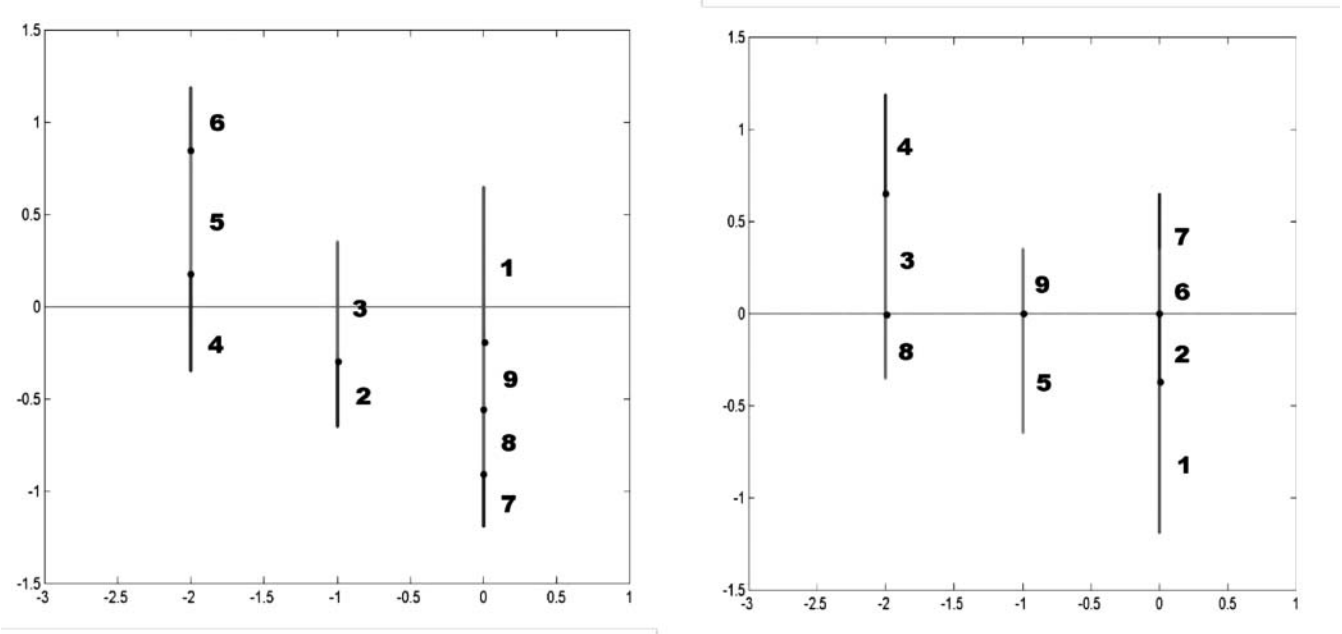

FIGURE 9. Projection onto $E_j \oplus E_{T,s}$. Here E_j is represented horizontally by only one dimension, since the projection is reduced to 3 points.

Theorem 5.4. *The adherence of the projection* $\Pi_{///}(\mathcal{V}^u)$ *is equal to* $\widehat{K}$. *The subsets* $\overline{\Pi_{///}(\mathcal{V}^{u,a})}$ *are disjoint intervals (up to measure zero).*

Proof: For $i \in \mathcal{A}$, let $k^-(i)$ be the index such that $I_i \subset K_{k^-(i)}$ and let $k^+(i)$ be such that $T(I_i) \subset K_{k^+(i)}$. It follows from analysis done in this section that $\Pi_j(e_i) = M_{k^+(i)} - M_{k^-(i)}$, while according to Lemma 9.3, $\Pi_{\overline{T},s}(e_i)$ is proportional to $t_i - \alpha_{k^+(i)} + \alpha_{k^-(i)}$. Hence, the same argument as in the proof of Lemma 4.4 but considering the K_i's as disjoint intervals establishes the result. □

The interpretation is that the projection to the subspace E_j corresponds to the segment K_i containing the point, while the projection onto $E_{\overline{T},s}$ is proportional to the distance from the point to the periodic point α_i (contained in K_i). This result stresses the importance of the partition we introduced, showing that the induction is better understood if we consider our map as defined on the union of the three intervals K_1, K_2, and K_3 instead of the circle. On the Rauzy fractal obtained here, the abelianization matrix acts as a contraction/permutation, the three intervals being shrunk around M_i and permuted.

6. THE UNSTABLE SUBSPACE

As we saw in Section 2.5, in the unstable subspace E_u there is no hope of constructing a Rauzy fractal, since the projection of the stepped line is unbounded, but we can describe the behavior of the projection of the stepped line using a renormalization procedure. The "renormalized" stepped line tends to a well-identified Peano curve filling a planar domain (with geometric properties close to those of the tribonacci fractal). Using properties of the neutral direction, we also give an interpretation of the McMullen curve as another projection of our stepped line having the same asymptotic properties.

6.1. Projection to the Antitribonacci Unstable Plane: The Discrete Stepped Line

We are interested in the unbounded stepped lines $\Pi_{\overline{T}}(\mathbf{L}^u)$ and $\Pi_{\overline{T},u}(\mathbf{L}^u)$. We are going first to describe some properties of these discrete stepped lines.

Theorem 6.1. *The stepped line* $\Pi_{\overline{T}}(\boldsymbol{L}^u)$ *is unbounded but remains within bounded distance of the plane* $E_{\overline{T},u}$. *It has multiple points of order not larger than 3.*

Proof: To see that it is not bounded, it is enough to exhibit an unbounded sequence of points, for instance the $\Pi_{\overline{T}}(x^u_{|\sigma^n(1)|})$. Since direction $E_{\overline{T},s}$ is contracting, bound-

edness in the direction transversal to $E_{\overline{T},u}$ is a consequence of Proposition 2.12. We observe that all points have integral coordinates (in a suitable basis). Hence they project to distinct points on the $E_{\overline{T},s}$ (irrational) axis (parallel to $E_{\overline{T},u}$). But no more than three points can have the same projection onto $E_{\overline{T},s}$ in view of Theorem 5.1 (one coming from each K_i); there are indeed multiple points of order up to 3. □

Remark 6.2. We mention without proof that the projection onto $E_{\overline{T},u}$ of this stepped line has no crossings. It is quite easy to see that no crossing can occur at the multiple points (it suffices to analyze words of length two giving rise to multiple points). It is more difficult to show, but it is nonetheless true, that two edges (between successive points) of the stepped line cannot cross; this is done in [Lowenstein et al. 07], and we could not do better than to duplicate their analysis.

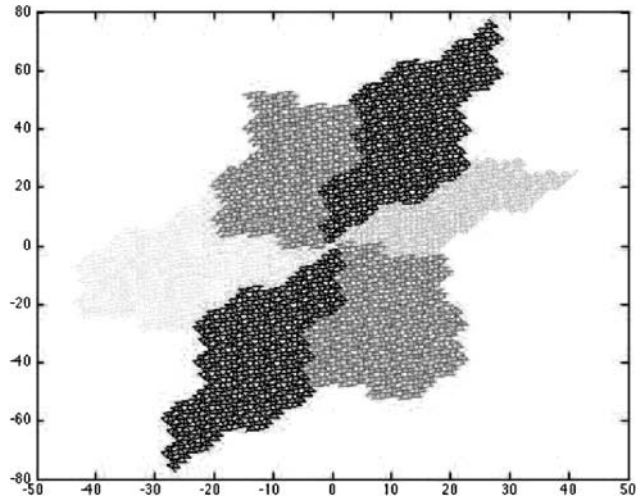

FIGURE 10. Long pieces of the stepped lines corresponding to the three positive fixed points and to the three negative fixed points.

The space E_n admits as basis $\{e_2 - e_3, e_5 - e_6, e_8 - e_9\}$; hence the projection onto $E_T \oplus E_{\overline{T}}$ gives the same image to e_2 and e_3, e_5 and e_6, e_8 and e_9; the projection onto the stepped line on this space is in fact the canonical stepped line associated with the substitution $\hat{\sigma}$. The projection onto $E_{\overline{T}}$ of the canonical stepped line associated with σ is also the projection of the stepped line associated with $\hat{\sigma}$.

When we draw the picture of the projection onto $E_{\overline{T},u}$ of the canonical stepped line associated with u, it seems to fill an approximate angular sector of the plane for a large number of points. The exact behavior can be understood completely; we give the results and omit the proof, which is straightforward but tedious.

We need first to consider the three infinite periodic points u, $u^{(2)}$, $u^{(3)}$; the corresponding stepped lines, which project almost to the same points in E_T, project to disjoint domains in $E_{\overline{T}}$, but this fills only half of the plane, in three disjoint angular sectors.

We also need to consider periodic left-infinite fixed points, indexed by negative integers. A small computation shows that there are two orbits of order 3: one consists of left-infinite periodic points ending in $2, 5, 8$, and the other in points ending in $3, 6, 9$. But it is easy to check that the left-infinite periodic point ending with 2 differs only in the last letter of the left-infinite periodic point ending with 3, and similarly for $5, 6$ and $8, 9$. Hence there are really only three stepped lines corresponding to left-infinite fixed points.

We can pair a right-infinite and a left infinite-periodic point to obtain a bi-infinite periodic point; but this makes sense from the viewpoint of symbolic dynamics only if the pair ab at the origin of the periodic point occurs in the language of the substitution, that is, in any sufficiently large image of a letter. An easy study shows that only six pairs can occur: $21, 53, 84$ and $61, 93, 34$.

If we draw the six stepped lines, the picture we obtain is striking (shown in Figure 10 for a large number of points). The three right-infinite periodic points alternate with the three left-infinite periodic points, each periodic point of one type being connected to the two neighboring periodic points of the other type, and they seem to fill the whole plane. We are going to prove that indeed, renormalizations of these stepped lines fill the plane.

Remark 6.3. The union of these six canonical lines is not exactly a cut-and-project scheme, but it is very close. If we fix one K_i and we consider only the points of type a such that $\rho(a) = i$, then every point in the slice $x + \alpha y + \alpha^2 z \in K_i - \alpha_i = [\beta_{i-1} - \alpha_i, \beta_i - \alpha_i]$ is obtained exactly once. Of course, points in the intersections of the slices can be obtained two or three times. Thus the union of lines appears as the superposition of three cut-and-project schemes with different (but overlapping) windows. It might seem easier to restrict to one of the K_i, but self-similarity would appear only by taking the cube of the induction. In some sense, that is the strategy developed in [Lowenstein et al. 07], except that since artificial importance is given to the point 0, induction is done on a smaller interval and self-induction occurs only after the induction interval is indeed "inside" K_1.

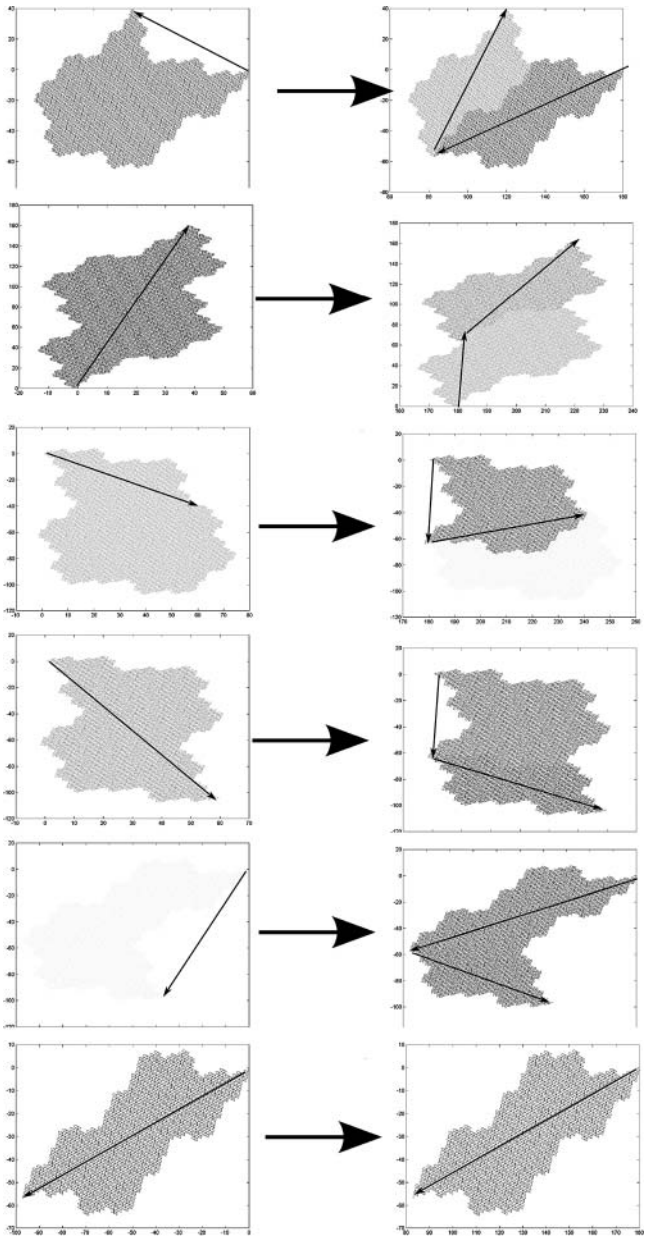

FIGURE 11. The IFS.

6.2. Unstable Plane in Antitribonacci: Renormalization

We consider the family of sequences of finite stepped lines defined, for all $a \in \mathcal{A}$, by

$$\widetilde{\mathbf{L}}_n^a = M^{-n}(\mathbf{L}^{\sigma^n(a)}).$$

Using the results of Section 2.5, we see that the projections onto the unstable space $\Pi_{\overline{T},u}(\widetilde{\mathbf{L}}_n^a)$ of these sequences converge to a curve $\mathcal{C}^a : [0; \Pi_{T,u}(e_a)] \to E_{\overline{T},u}$. For all n and all $0 \le k \le \sigma^n(a)$, if $t_k^{(n)} = \alpha^n \Pi_{T,u}(M^{-n} x_k^{\sigma^n(a)})$, we have $\mathcal{C}^a(t_k^{(n)}) = \Pi_{\overline{T},u}(M^{-n} x_k^{\sigma^n(a)})$. We call the compact subsets $\mathcal{R}_a^* = \mathcal{C}^a([0; \Pi_{T,u}(e_a)])$ *elementary tiles*.

Theorem 6.4. *The compact sets $\{\mathcal{R}_a^*, a \in \mathcal{A}\}$ satisfy the system of set equations (6–1) below. As subsets of the plane, each $\mathcal{R}_a^*$ has nonempty interior.*

Proof: First we make explicit the GIFS. Then, we prove that a particular union of translates of the tiles satisfies the same GIFS as the tribonacci fractal.

The GIFS is an immediate consequence of Proposition 2.22. There is a slight simplification: $\mathcal{R}_2^* = \mathcal{R}_3^*$, $\mathcal{R}_5^* = \mathcal{R}_6^*$, and $\mathcal{R}_8^* = \mathcal{R}_9^*$, since the corresponding projections are equal ($\Pi_{\overline{T},u}(e_2) = \Pi_{\overline{T},u}(e_3), \dots$), and the images are also equal modulo this identification. We obtain the system of set equations

$$\begin{aligned}
\mathcal{R}_1^* &= M^{-1}\mathcal{R}_2^* \cup (M^{-1}\Pi_{\overline{T},u}(e_2) + M^{-1}\mathcal{R}_5^*),\\
\mathcal{R}_2^* &= M^{-1}\mathcal{R}_4^* \cup (M^{-1}\Pi_{\overline{T},u}(e_4) + M^{-1}\mathcal{R}_5^*),\\
\mathcal{R}_4^* &= M^{-1}\mathcal{R}_1^* \cup (M^{-1}\Pi_{\overline{T},u}(e_1) + M^{-1}\mathcal{R}_7^*),\\
\mathcal{R}_5^* &= M^{-1}\mathcal{R}_1^* \cup (M^{-1}\Pi_{\overline{T},u}(e_1) + M^{-1}\mathcal{R}_8^*),\\
\mathcal{R}_7^* &= M^{-1}\mathcal{R}_2^* \cup (M^{-1}\Pi_{\overline{T},u}(e_2) + M^{-1}\mathcal{R}_8^*),\\
\mathcal{R}_8^* &= M^{-1}\mathcal{R}_\cdot^*
\end{aligned} \tag{6–1}$$

Let $W = 825$. We claim that the union of tiles $\mathcal{R}_W^* = \mathcal{R}_8^* \cup (\Pi_{\overline{T},u}(e_8) + \mathcal{R}_2^*) \cup (\Pi_{\overline{T},u}(e_8 + e_2) + \mathcal{R}_5^*)$ is a tribonacci fractal. We observe that $\sigma^3(W) = 17183529352461845$. Identifying $2 \cong 3$, $5 \cong 6$, and $8 \cong 9$, we write $\hat{\sigma}^3(W) = \hat{\sigma}^2(25)(825)\hat{\sigma}(825)\hat{\sigma}^2(8)$.

Set $z = \Pi_{\overline{T},u}(e_{\sigma^2(25)}) = \Pi_{\overline{T},u}(e_{1718352})$. Note that we have the equalities $\Pi_{\overline{T},u}(e_W) = \Pi_{\overline{T},u}(e_{\sigma(W)}) = \Pi_{\overline{T},u}(e_{\sigma^2(W)}) = 0$, whence $\Pi_{\overline{T},u}(e_{\sigma^2(25)}) + \Pi_{\overline{T},u}(e_{\sigma^2(8)}) = 0$. We obtain, using the cyclic decomposition of $\hat{\sigma}^3(W)$,

$$\begin{aligned}
&\Pi_{\overline{T},u}(\mathcal{V}^{\sigma^3(W)})\\
&\quad = \Pi_{\overline{T},u}(\mathcal{V}^{\sigma^2(25)}) \cup (z + \Pi_{\overline{T},u}(\mathcal{V}^W))\\
&\qquad \cup (z + \Pi_{\overline{T},u}(\mathcal{V}^{\sigma(W)})) \cup (z + \Pi_{\overline{T},u}(\mathcal{V}^{\sigma^2(8)}))\\
&\quad = (z + \Pi_{\overline{T},u}(\mathcal{V}^W)) \cup (z + \Pi_{\overline{T},u}(\mathcal{V}^{\sigma(W)}))\\
&\qquad \cup (z + \Pi_{\overline{T},u}(\mathcal{V}^{\sigma^2(8)}))\\
&\qquad \cup (z + \Pi_{\overline{T},u}(e_{\sigma^2(8)}) + \Pi_{\overline{T},u}(\mathcal{V}^{\sigma^2(25)}))\\
&\quad = (z + \Pi_{\overline{T},u}(\mathcal{V}^W)) \cup (z + \Pi_{\overline{T},u}(\mathcal{V}^{\sigma(W)}))\\
&\qquad \cup (z + \Pi_{\overline{T},u}(\mathcal{V}^{\sigma^2(W)})).
\end{aligned}$$

We deduce, applying σ^n and M^{-n}, and letting $n \to \infty$, that

$$\mathcal{R}_W^* = z + (M^{-3}\mathcal{R}_W^* \cup M^{-2}\mathcal{R}_W^* \cup M^{-1}\mathcal{R}_W^*).$$

Recalling that the action of M^{-1} on $E_{\overline{T},u}$ is conjugate to a similarity of ratio μ, as is the action of M in

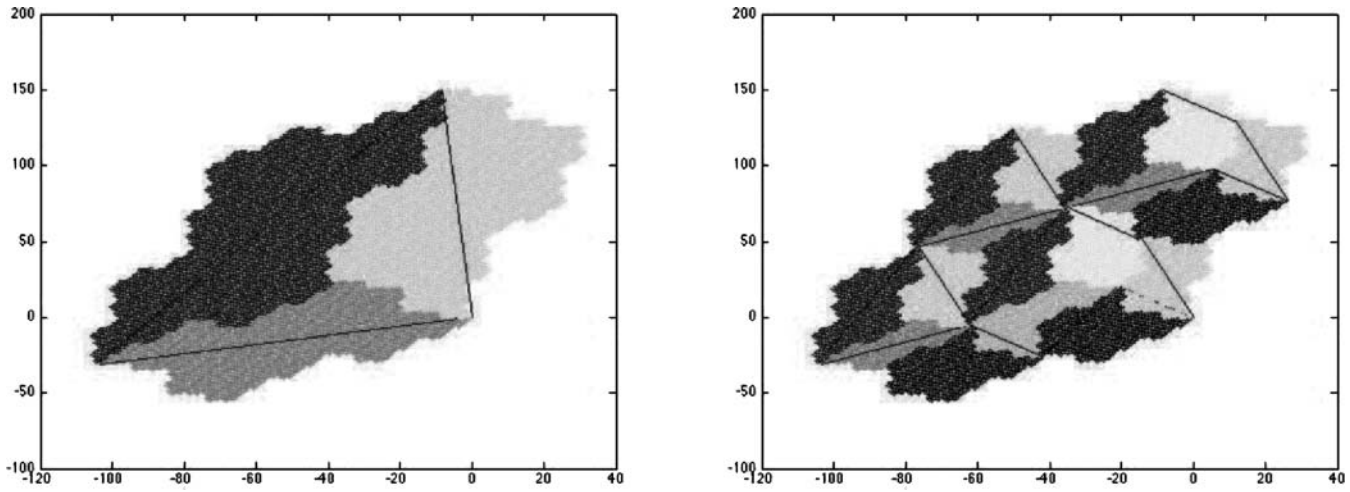

FIGURE 12. The set $\mathcal{R}_W^*$ decomposed into elementary tiles 825 and at level 3 into elementary tiles 17183529352461845.

the stable plane, we see that the unique solution of this set equation, up to a similitude, is the tribonacci fractal. This result shows that at least one of the tiles $\mathcal{R}_8^*$, $\mathcal{R}_2^*$, $\mathcal{R}_5^*$ has nonempty interior. It then follows, by an obvious primitivity argument, that all tiles have nonempty interior. □

Remark 6.5. The argument used in the proof shows that some pieces of the boundaries of the tiles coincide with pieces of boundaries of the tribonacci fractal. A more careful combinatorial analysis would be required to understand exactly the structure of the boundary. But this sheds some light on the result obtained in [Lowenstein et al. 07] about the dimension of the boundaries of the domains filled by the McMullen curve.

Remark 6.6 Observe that the occurrence of the tribonacci fractal in this construction is somehow unexpected. We cannot hope for such coincidence for general substitutions, since the action of M on the contracting space has no reason to be conjugate to the action of M^{-1} on the expanding space. A necessary condition is the reciprocity of the characteristic polynomial. This is true for geometric reasons in the case of self-induced IET coded by continuity intervals. We do not know whether it is always sufficient in the general case.

6.3. The McMullen Discrete Curve

Definition 6.7. We denote by Q the bijection from $\mathbb{Z}^3$ onto $\frac{1}{2}\mathbb{Z}[\alpha]$ defined by

$$Q(n,p,q) = \frac{n}{2} + \frac{p}{2}\alpha + \frac{q}{2}\alpha^2.$$

The set $\mathcal{Z} = Q^{-1}(\frac{1}{2}\mathbb{Z}[\alpha] \cap [\beta_0, \beta_3[)$ is a "slice" in $\mathbb{Z}^3$ between two planes. It is partitioned in two cosets, depending on whether the parity of $n+p+q$ is odd or even, which are exchanged by the involution $I_{[\beta_0,\beta_3[} : x \mapsto x + 1/2 \mod 1$ on the interval. Each coset is in correspondence with $\mathbb{Z}^2$ by the following trivial lemma:

Lemma 6.8. *The map $\mathcal{Z} \to \mathbb{Z}^2$, $\frac{n}{2} + \frac{p}{2}\alpha + \frac{q}{2}\alpha^2 \mapsto (p,q)$, is two-to-one, since for all $(p,q) \in \mathbb{Z}^2$ there is a unique n such that $Q(n,p,q) \in [\beta_0,\beta_3)$, $Q(n+1,p,q) \in [\beta_0,\beta_3)$, i.e., exactly two points in the slice. It is one-to-one on each coset of a given parity.*

Definition 6.9. We call the stepped line that admits the lift to $\mathbb{Z}^3$ of the orbit of the fixed point α_1, $(Q^{-1}(T^n(\alpha_1)))_{n\geq 0}$ as an ordered sequence of vertices the *McMullen curve*, and we denote it by $\mathcal{L}$.

We see that $\mathcal{L}$ is a stepped line because the differences $Q^{-1}(T^{n+1}(\alpha_1)) - Q^{-1}(T^n(\alpha_1))$ are given by $Q^{-1}(t_{u_n})$, and it is the image of the stepped line $\mathbf{L}^u$ by the map $e_a \mapsto Q^{-1}(t_a)$, for $a \in \mathcal{A}$.

This stepped line is a piece of a more complete object: a family of stepped lines that partition the slice $\mathcal{Z}$. Let z be any point in $\mathcal{Z}$. Since $Q(z) \in [\beta_0,\beta_3[$, we can set $\mathcal{T}(z) = Q^{-1}(T(Q(z)))$. This defines a map from $\mathcal{Z}$ to itself, and by construction, $\mathcal{T}(z) - z$ takes values in the finite set $\{Q^{-1}(t_a), a \in \mathcal{A}\}$. Hence through any point z_0 in $\mathcal{Z}$ there passes a bi-infinite stepped line $(z_n)_{n\in\mathbb{Z}}$ connecting z_n to $z_{n+1} = \mathcal{T}(z_n)$. The sets of vertices of these stepped lines are infinite, since by minimality, the IET has no periodic points. This family of curves is well understood:

Proposition 6.10. *Each of these stepped lines is contained in a coset of fixed parity. The odd coset is the disjoint union of the three stepped lines through the points* $Q^{-1}(\alpha_1)$, $Q^{-1}(\alpha_2)$, $Q^{-1}(\alpha_3)$*; the stepped line* $\mathcal{L}$ *is the "positive half" of one of these, namely the one starting at* $Q^{-1}(\alpha_1)$*. The even coset is the disjoint union of the image of these three stepped lines by the involution* $I_{[\beta_0,\beta_3[}$.

Proof: Parity is preserved along a stepped line, since elementary moves do not change it. Hence each stepped line is contained in one coset. The projection onto the last two coordinates then becomes one-to-one, and we obtain a picture in $\mathbb{Z}^2$.

The involution $I_{[\beta_0,\beta_3)}$ conjugates T to T^{-1}. Hence, the image of a stepped line by this involution is a stepped line in the other coset, which projects to the same stepped line in $\mathbb{Z}^2$, with opposite orientation.

We claim that there are exactly six distinct bi-infinite stepped lines (three in the odd coset and three in the even coset) covering all $\mathcal{Z}$. Figure 13 shows how the three even stepped lines behave close to the origin. Figure 14 shows the "positive" halves of the same three stepped lines seen at a larger scale. Let us give an idea of the argument, similar to the one developed in [Lowenstein et al. 07].

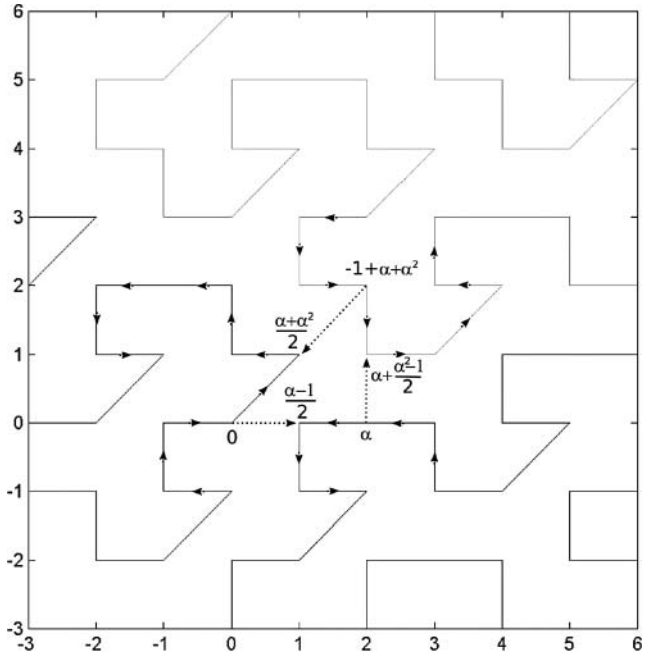

FIGURE 13. Projection onto $\mathbb{Z}^2$ of three stepped lines corresponding to forward orbits of 0, α, and $-\alpha^3$. Dotted arrows correspond to the other possibilities at the singularities (if the intervals were left open instead of being left closed in the definition of the IET. Points represented correspond to points $(n, p, q) \in \mathcal{Z}$ with $n + p + q$ even.

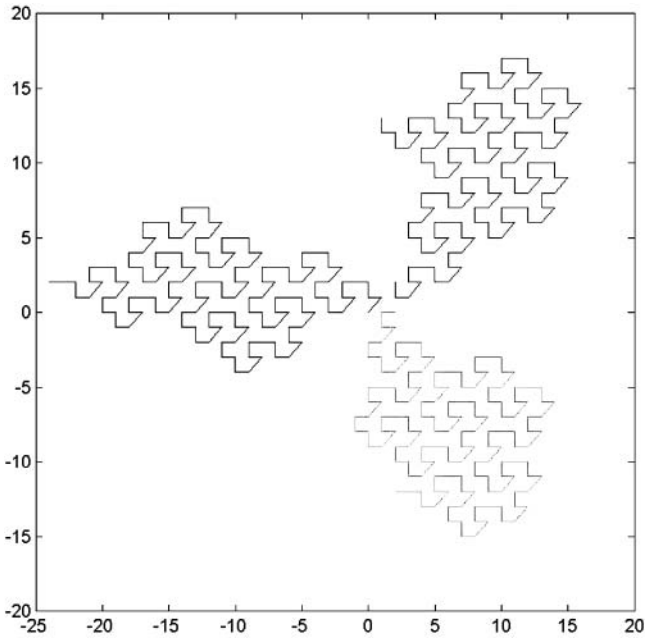

FIGURE 14. The McMullen curves corresponding to forward orbits of the three fixed points. Projection onto $\mathbb{Z}^2$.

Consider a point $z_0 \in \mathcal{Z}$ that is in the odd coset, and denote by L_0 the stepped line going through z_0. Since the return time to any interval of positive measure is bounded, there is a constant C (independent of z_0) such that there is a point $z_0' \in L_0$ with $Q(z_0') \in J_a$ and $\|z_0 - z_0'\| < C$. Set $z_1 = M^{-1}z_0'$. Since $Q(z_0') \in J_a$, $z_1 \in \mathcal{Z}$. Moreover, $\|z_1\| \leq |\mu|(\|z_0\| + C)$. There is a constant B ($B = 2C/(1 - |\mu|)$) such that iterating this procedure, we end up (after finite time for all initial z_0) in the ball of radius B. A direct computation shows that the intersection of the odd coset with the ball of radius B contains only stepped lines issued from a fixed point. Using the self-similarity of these lines, we can go back to z_0 to deduce that it was in such a stepped line. Hence the odd coset is partitioned by the stepped lines corresponding to the three periodic points, and the even coset by their images under the involution. □

It is delicate (but done in [Lowenstein et al. 07]) to prove that there are no crossings (neither self-crossings nor crossings between two of the three stepped lines of a class) in the planar projections (onto $\mathbb{Z}^2$ and onto the "stable" plane). A combinatorial analysis of the finite number of possibilities provides a proof. It follows from this last statement that a renormalization of the three

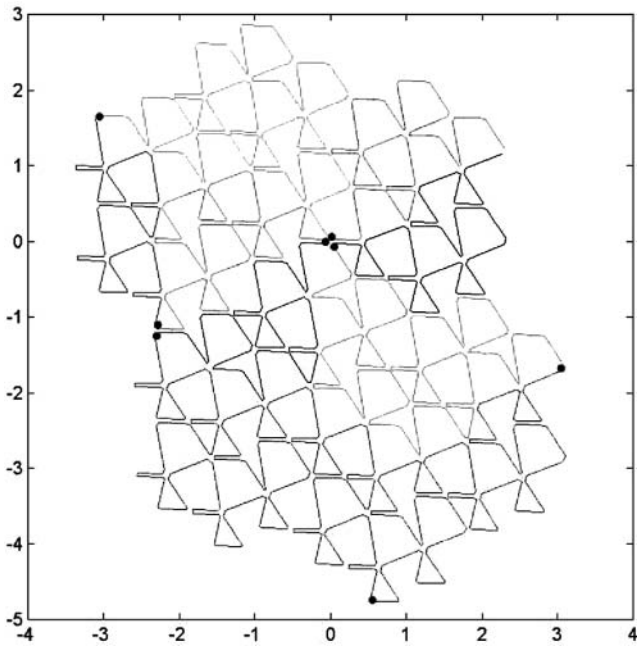

FIGURE 15. A view of $\Pi^*_{\overline{T},u}(M^{-6}\mathcal{V}^{\sigma^6(W)})$. Multiple points have been artificially split to allow one to "follow" the curve. Dots separate pieces corresponding to images of the different letters.

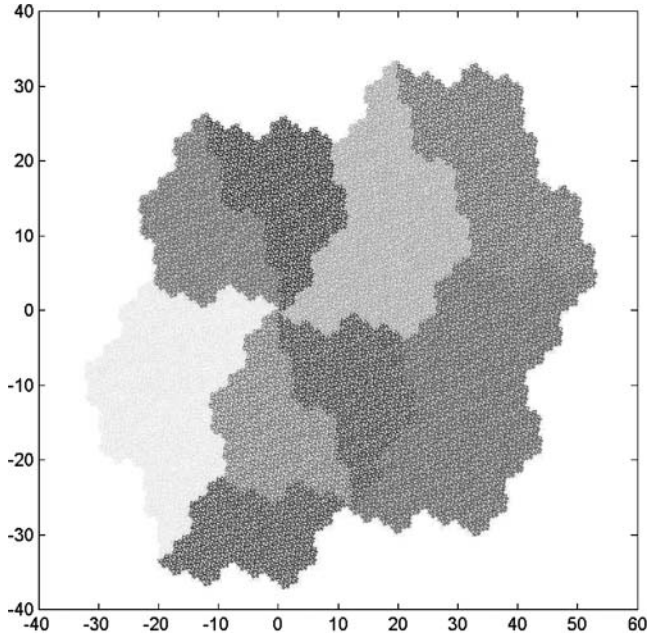

FIGURE 16. The limiting space-filling curve $\lim_{N\to\infty}\Pi^*_{\overline{T},u}(M^{-N}\mathcal{V}^{\sigma^N(W)})$.

stepped lines of a class must fill the plane with three (essentially disjoint) subsets. We will be able to give a precise description of the boundaries of these domains (there was an attempt in [Lowenstein et al. 07]).

Since ${}^tA^{-1}$ is the companion matrix of the minimal polynomial of α, we have $\alpha Q(v) = Q({}^tA^{-1}v)$. Hence multiplication by α seen in $\mathcal{Z}$ splits into a contraction in the direction $(1, \alpha, \alpha^2)$ and an expansion (conjugate to a similarity of ratio β) in the plane $x + \alpha y + \alpha^2 z = 0$. We will see that it is rather natural to project the McMullen stepped lines onto this plane.

Remark 6.11. We propose a still more general construction, similar to what is done in [Lowenstein et al. 07]. Starting with a given point in $x \in [\beta_0, \beta_3)$, we consider in $\mathbb{Z}^3$ the bi-infinite stepped line defined by $z_0 = 0$ and, for all $n \in \mathbb{Z}$, $z_{n+1} - z_n = Q^{-1}(T^{n+1}(x)) - Q^{-1}(T^n(x))$. We claim that generically, the projection of this stepped line onto $\mathbb{Z}^2$ fills $\mathbb{Z}^2$; for a countable set of points (the orbit of the discontinuities), there are three stepped lines, and for an uncountable set of Lebesgue measure zero, there are two stepped lines.

This is reminiscent of the structure of the space of Penrose tilings, where some special tilings have symmetry of order 2 or 10, and generic tilings do not have these symmetries.

We now prove that the *McMullen curve* $\mathcal{L}$ can be interpreted as yet another projection (up to a translation) of the stepped line $\mathbf{L}^u$. It will be convenient to generalize the map Q to any three-dimensional lattice with a fixed basis.

Definition 6.12. Let E be a 3-dimensional vector space with a basis $\mathcal{B}$. We define the map $Q_{E,\mathcal{B}}$, from the lattice generated by $\mathcal{B}$ to $\frac{1}{2}\mathbb{Z}[\alpha]$, by $Q_{E,\mathcal{B}}(v) = \frac{n}{2} + \frac{p}{2}\alpha + \frac{q}{2}\alpha^2$ if v has coordinates (n, p, q) in the basis $\mathcal{B}$.

We use the basis $\hat{\mathcal{B}}$ defined in Section 9.2, and the projection $\hat{\Pi}$ to $E_{\overline{T}}$ defined in that section by $\hat{\Pi} = \Pi_F \circ (\Pi_j \oplus \Pi_{\overline{T}})$, where Π_F keeps invariant the basis $\{\hat{e}_4, \hat{e}_5, \hat{e}_6\}$ of $E_{\overline{T}}$, sends E_T to 0, and sends $\hat{e}_i$ to $\hat{e}_{i+3}$ for $i = 1, 2, 3$. We view this projection $\hat{\Pi}$ as a map from $\mathbb{R}^{\mathcal{A}}$, endowed with the canonical basis, to $E_{\overline{T}}$, endowed with the basis $\{\hat{e}_4, \hat{e}_5, \hat{e}_6\} \subset \hat{\mathcal{B}}$, and we identify in this way $E_{\overline{T}}$ and $\mathbb{R}^3$.

Theorem 6.13. *We have*

$$\hat{\Pi}(\boldsymbol{L}^u) = \mathcal{L} - Q^{-1}(\alpha_1).$$

Proof: This equality makes sense, since $\hat{\Pi}(\mathbf{L}^u)$ is contained in $E_{\overline{T}}$ and $\mathcal{L}$ is included in $\mathbb{R}^3$, and we have identified these two spaces. It is a direct consequence of Lemma 9.3. Indeed, by definition, successive points in $\hat{\Pi}(\mathbf{L}^u)$ satisfy

$$\hat{\Pi}(x^u_{n+1}) = \hat{\Pi}(x^u_n) + \hat{\Pi}(e_{u_n}),$$

while successive points in $\mathcal{L}$ satisfy

$$Q^{-1}(T^{n+1}(\alpha_1)) = Q^{-1}(T^n(\alpha_1)) + Q^{-1}(t_{u_n}).$$

But Lemma 9.3 asserts that $\hat{\Pi}(e_a) = Q^{-1}_{E_{\overline{T}},\hat{\mathcal{B}_{\overline{T}}}}(t_a)$; hence the two lines have the same increments. The theorem follows immediately from the fact that the line $\hat{\Pi}(\mathbf{L}^u)$, by definition, begins at the origin, while $\mathcal{L}$ begins at $Q^{-1}(\alpha_1)$. □

It happens that this stepped line is very close to the projection $\Pi_{\overline{T}}$ of the stepped line $\mathbf{L}^u$ onto the space $E_{\overline{T}}$, the difference being related to what happens in the "neutral" direction. To make this dependence more explicit, let us now define a piecewise translation from $\mathbb{Z}^3$ (as the space of the McMullen curve) to $\mathbb{Z}^3$ (as the space $E_{\overline{T}}$), by

$$K(z) = z - \sum_{i=1}^{3} Q^{-1}(\alpha_i)\mathbf{1}_{K_i}(Q(z)). \qquad (6\text{–}2)$$

Observe that $K(\mathcal{L})$ is also a stepped line, since the number of possible translations is finite, and indeed, we have the following result:

Theorem 6.14.

$$\Pi_{\overline{T}}(\boldsymbol{L}^u) = K(\mathcal{L}).$$

Proof: We observe that for all i and all $z \in \mathcal{Z}$ with $Q(z) \in K_i$, $Q(K(z)) = Q(z) - \alpha_i$. It follows from Theorem 6.13 and from the proof of Theorem 5.1 that

$$\begin{aligned} T^n(\alpha_1) &= \sum_{i=1}^{n} Q(\Pi_{\overline{T}}(e_{u_i}) + \Pi_j(e_{u_i})) \\ &= Q(\Pi_{\overline{T}}(x^u_n)) - \alpha_{k^-(u_n)}. \end{aligned}$$

□

This result shows that it is possible to switch from $\mathbf{L}^u$ to $\mathcal{L}$ by moving points by (uniformly bounded) translations. It is worth observing that by definition, the McMullen curve has no multiple points. Hence these "translations" do split the multiple points of $\mathbf{L}^u$. Of course the advantage of $\mathbf{L}^u$ is that its self-similarity properties are much simpler than those of the McMullen curve. As we will see in the next section, since the two curves remain at bounded distance, the limiting Peano curves are the same.

6.4. The Renormalized McMullen Curve

We define the concatenation of two Peano limit curves $\mathcal{C}^a$ and $\mathcal{C}^b$ (defined as in Section 6.2) as the Peano limit curve obtained from ab, denoted by $\mathcal{C}^{ab}$. We naturally extend this notation to unbounded curves associated with infinite words.

The stepped line $\mathcal{L}$ is somehow self-similar. But the self-similarity at finite scales is not completely obvious, and the easiest way to analyze the limiting rescaled curve is to compare it with $\Pi_{\overline{T},u}(\mathcal{V})$. Assume that we have a parameterization of $\mathcal{L}$, that is, a bijective map φ from $\mathbb{R}^+$ onto the union of the segments joining successive points of $\mathcal{L}$. Define the map Π_α as the projection onto the unstable plane of the matrix A along its stable line. We call the limiting curve

$$\widetilde{\mathcal{L}}(t) = \lim_{n\to\infty} \Pi_\alpha({}^tA^{-3n}\varphi(\alpha^{-3n}t))$$

the *renormalized McMullen curve*.

This limiting curve is well defined, and is exactly $\mathcal{C}^u$.

Theorem 6.15. *The renormalized projection of the McMullen curve tends to a space-filling curve $\widetilde{\mathcal{L}}$ that is equal to the Peano curve $\mathcal{C}^u$.*

Proof: Formally, this result is a consequence of Theorem 9; indeed, since the two stepped lines remain at uniformly bounded distance, their renormalization by similarity must have the same limit. A natural parameterization for the McMullen curve is obtained by taking the natural one for the projection $\mathcal{L} = \hat{\Pi}(\mathbf{L}^u)$, giving length $\Pi_{\overline{T},u}(e_a)$ to a step in direction e_a. □

The idea behind this proof is that what happens in the neutral direction vanishes in the limit because of the contraction. But at finite stages the identifications $2 \cong 3$, $6 \cong 7$, and $8 \cong 9$ do not hold for the McMullen curve, so a complete formalization would be difficult, as would be a direct study of the McMullen curve. In other words, the projection of the McMullen curve onto the plane $E_{\overline{T},u}$ is obtained by a projection $\Pi_{\overline{T},u} \circ \hat{\Pi}$ that does not commute with M but is such that the conjugates $M^{-n}\Pi_{\overline{T},u}\hat{\Pi}M^n$ converge to the projection $\Pi_{\overline{T},u}$.

Remark 6.16 The union of the renormalizations of the three McMullen curves fills the plane, and a more specific analysis of their shape follows from analysis of the space-filling curves $\mathcal{C}^a$.

7. THE DUAL SUBSPACE

7.1. Dual Substitution

We consider the following substitution, called *dual substitution* of σ:

$$\begin{aligned}\sigma_* : 1 &\to 456\\ 2 &\to 78\\ 3 &\to 91\\ 4 &\to 23\\ 5 &\to 12\\ 6 &\to 3\\ 7 &\to 4\\ 8 &\to 5\\ 9 &\to 67.\end{aligned}$$

Its matrix is the transpose ${}^tM$ of M. The choice of the ordering is given by the way the continuity intervals of T are ordered on the interval. Indeed, this substitution describes the way the dynamical partition splits after induction. We stress again that there is no clear definition of such a "dual" substitution without the help of the geometry of the underlying IET.

We decompose $\mathbb{R}^{\mathcal{A}}$ into three stable subspaces, E^*_n, E^*_T, and $E^*_{\overline{T}}$ (with the natural notation for the corresponding projections). The relation $M = P^{-1}BP$ transposes into ${}^tM = {}^tP\,{}^tB\,{}^tP^{-1}$. Hence basis vectors for the stable spaces can be taken to transposes of row vectors of P^{-1}. We observe that σ_* has six periodic points (of period 3), respectively limits of $\sigma_*^{3n}(4)$, $\sigma_*^{3n+1}(4) = \sigma_*^{3n}(2)$, $\sigma_*^{3n+2}(4) = \sigma_*^{3n}(7)$, and $\sigma_*^{3n}(3)$, $\sigma_*^{3n+1}(3) = \sigma_*^{3n}(9)$, $\sigma_*^{3n+2}(3) = \sigma_*^{3n}(6)$.

We could have done various things to study the stepped line(s) associated with this substitution. But we decided to focus on its projection onto the unstable space $E^*_{\overline{T}}$ because we recover the Peano curve obtained in [Arnoux 88] (and by ourselves in Section 4.5) as limit Peano curve of a sequence of renormalized stepped lines. This indeed provides an IFS construction of the curve, and this question has been one of the starting points of this work.

7.2. Unstable Space in Dual Antitribonacci

The space $E^*_{\overline{T},u}$ is the unstable space associated with the eigenvalues β and $\overline{\beta}$ of the matrix ${}^tM$. In this subspace, it makes sense to use the theory developed in Section 2.5 to investigate the stepped lines $\Pi^*_{\overline{T},u}(M^{-N}(\mathbf{L}^{\sigma_*^N(a)}))$ for $a \in \mathcal{A}$ and their limiting curves $\mathcal{C}^a_*$. To illustrate the link with [Arnoux 88], we want to show how the circle $\mathbb{S}^1$ can be naturally embedded in a tribonacci fractal using these limiting curves.

For all $a \in \mathcal{A}$ we can view $\mathcal{C}^a_*$ as a map defined on I_a. Concatenation of the stepped lines (as in Section 6.4) in the order 789123456 would yield a map defined on $\mathcal{I}$, and our point is that its image is a tribonacci fractal. For technical reasons it is more convenient to state the result using the order prescribed by the image partition $T(\mathcal{I})$ and to move the origin; we consider the concatenation of the curves in the order $W = 341267598$. In this setting, the fixed points are at the boundaries of the intervals, and they are mapped onto the origin.

If we define $e_a = -\Pi^*_{\overline{T},u}(e_7)$, $e_b = \Pi^*_{\overline{T},u}(e_1)$, $e_c = -\Pi^*_{\overline{T},u}(e_4)$, we obtain a basis of the 3-dimensional space $E^*_{\overline{T},u}$, which can be viewed as $\mathbb{R}^{\breve{\mathcal{A}}}$, on which ${}^tM^{-1}$ acts as A; the tribonacci fractal $\breve{\mathcal{R}}$ can be embedded in this way into $E^*_{\overline{T},u}$.

Theorem 7.1. *In* $E^*_{\overline{T},u}$,

$$\mathcal{R}^*_W := \lim_{N\to\infty} (\Pi^*_{\overline{T},u}({}^tM^{-N}\mathcal{V}^{\sigma_*^N(W)})) = \breve{\mathcal{R}}.$$

The limiting curve is a space-filling curve filling precisely the tribonacci Rauzy fractal. This result could be proved using the GIFS strategy already developed, for instance showing that it satisfies the characteristic system of set equations of the tribonacci Rauzy fractal. We adopt here a different strategy in order to illustrate the relation between the dual substitution and the substitution itself: we want to show that the "contraction" procedure for σ and the "expanding" procedure for σ_* both yield representations of $\mathbb{S}^1$ (in fact, of three pieces of the stable manifold of the pseudo-Anosov map underlying the induction).

Proof: We consider a point $x \in \mathbb{S}^1$. We propose to describe it in two ways: on the one hand, by following its symbolic dynamics (driven by the substitution σ), and on the other hand, by computing, at each level of refinement of the dynamical partition (driven by σ_*), the interval to which it belongs. These two symbolic descriptions yield two infinite sequences of prefixes for σ and σ_* (which happen to be paths with opposite orientations in the same graph by a general argument). The "contracting" construction (Section 2.4) for the substitution σ and the "expanding" construction (Section 2.5) for the dual substitution σ_* yield two maps from $\mathbb{S}^1$ to $\mathbb{R}^3$. The amazing fact is that these maps are the same (provided the bases are chosen correctly). Observe that there are two

dualities involved here. Indeed, we already observed that the "contracting" and "expanding" procedures yield dual GIFS (GIFS with transposed matrices), while we apply those dual procedures respectively to σ and to its dual σ_*.

Let us be more specific. Let $x \in \mathbb{S}^1$ and set $v = \varphi_{\mathcal{I}}(x)$. It is standard to associate to x an infinite path in the prefix automaton of σ. Here, this path is determined by the sequence of vertices $(a_n)_{n\geq 0}$ and related to the symbolic dynamics as follows: for all $n \geq 0$, $\sigma(a_{n+1}) = P_n a_n S_n$, while $v = \lim_{n\to\infty} S_0\sigma(S_1)\cdots\sigma^n(S_n)$. Observe that $\sigma^n(a_n) = \sigma^{n-1}(P_{n-1})\cdots\sigma(P_1)P_0a_0S_0\sigma(S_1)\cdots\sigma^{n-1}(S_{n-1})$. We consider the sequence of labels $(P_n)_{n\geq 0}$.

We observe that a_0 is the index of the interval of the partition $T(\mathcal{I})$ in which x lies. Let us consider the (unique) prefix $P^W_{a_0}$ of the word $W = 341267598$ such that $P^W_{a_0}a_0S^W_{a_0} = W$ for some suffix $S^W_{a_0}$ (that is, the list of the names of the intervals of $T(\mathcal{I})$ lying between α_3 and the interval containing x). The induction yields successive refinement of the partition $T(\mathcal{I})$ comprising intervals of the form $T^k(h^n(I_b))$ (at level n, for k integers and $b \in \mathcal{A}$), called intervals of type b.

At each level, an interval of type a is tiled by intervals of the next level, of types given (in the right order) by $\sigma_*(a)$ (by construction of σ_*). We observe that a_n is the type of the interval to which x belongs at level n. Since each letter appears at most once in each image, we can decompose $\sigma_*(a_{n-1}) = P^*_{n-1}a_nS^*_{n-1}$. It determines a sequence $(P^*_n)_{n\geq 0}$ of prefixes that is the sequence of labels of a backward path in the prefix automaton of σ_* (and indeed of the same path seen in the reverse direction). The position of x in the partition $T(\mathcal{I})$ is determined by the sequence $P^W_{a_0}, P^*_0, \ldots, P^*_n, \ldots$ in the sense that at level n, the word $\sigma^n_*(W)$ gives the list of the types of the intervals of level n tiling $\mathbb{S}^1$ (starting at α_3), and the decomposition

$$\sigma^n_*(W) = \sigma^n_*(P^W_{a_0})\sigma^{n-1}_*(P^*_0)\cdots P^*_{n-1}a_nS^*_{n-1} \cdots\sigma^{n-1}_*(S^*_0)\sigma^n_*(S^W_{a_0})$$

specifies the position of the copy of $h^n(I_{a_n})$ containing x.

We are going to use these two sequences $(P_n)_{n\geq 0}$ and $(P^*_n)_{n\geq 0}$ of prefixes to build two natural maps valued in $E_{T,s}$ and in $E^*_{\overline{T},u}$ respectively.

On the one hand, using the sequence $(P_n)_{n\geq 0}$, we define a map on $\mathbb{S}^1$ following the "contracting" construction proposed in Section 2.4. Consider the projections on $E_{T,s}$ of the (finite) stepped lines associated with $\sigma^n(P_n)\cdots\sigma(P_1)P_0a_0$. By the same arguments as those of Proposition 3, this sequence converges. We set

$$Y(x) = \Pi_{T,s}e_{a_0} + \sum_{i\geq 0} M^i.\Pi_{T,s}e_{P_i}.$$

On the other hand, following the procedure developed in Section 2.5, we associate to the sequence $(P^*_n)_{n\geq 0}$ a point in the limiting curve $\mathcal{C}^W_*$ by

$$Y^*(x) = \Pi^*_{\overline{T},u}e_{P^W_{a_0}} + \sum_{n\geq 0} {}^tM^{-n-1}\Pi^*_{\overline{T},u}e_{P^*_n}.$$

Let us identify E_T and $E^*_{\overline{T}}$ with $\mathbb{R}^{\breve{\mathcal{A}}}$ by the maps

$$\begin{aligned}\Pi : E_T &\to \mathbb{R}^{\breve{\mathcal{A}}},\\ \Pi_T(e_1) &\mapsto e_{,}\\ \Pi_T(e_5) &\mapsto e_b,\\ \Pi_T(e_8) &\mapsto e_c,\end{aligned}$$

and

$$\begin{aligned}\Pi^* : E^*_{\overline{T}} &\to \mathbb{R}^{\breve{\mathcal{A}}},\\ \Pi^*_{\overline{T}}(e_7) &\mapsto -e_a,\\ \Pi^*_{\overline{T}}(e_1) &\mapsto e_b,\\ \Pi^*_{\overline{T}}(e_4) &\mapsto -e_c.\end{aligned}$$

We observe that in the basis of E_T (respectively of $E^*_{\overline{T}}$), the matrix M (respectively ${}^tM^{-1}$) acts as the tribonacci matrix, i.e., $\Pi M = A\Pi$ (respectively $\Pi^{*t}M^{-1} = A\Pi^*$). We have the following:

Proposition 7.2. *For all $x \in \mathbb{S}^1$,*

$$\Pi(Y(x)) = \Pi^*(Y^*(x)).$$

We denote by $\breve{\Pi}_s$ the projection of $\mathbb{R}^{\breve{\mathcal{A}}}$ onto the stable plane of A parallel to the expanding direction. We observe that $\breve{\Pi}_s\Pi = \Pi\Pi_{T,s}$ on E_T and that $\breve{\Pi}_s\Pi^* = \Pi^*\Pi^*_{\overline{T},u}$ on $E^*_{\overline{T}}$. Recalling that $\Pi_{T,s}e_i = \Pi_{T,s}e_j$ as soon as $\rho(i) = \rho(j)$, we obtain, as in Theorem 4.1,

$$\Pi Y(x) = \breve{\Pi}_s e_{\rho(a_0)} + \sum_{i=0}^{\infty} A^i\breve{\Pi}_s e_{\rho(P_i)}.$$

For all $a \in \mathcal{A}$, we define $w_a = \Pi\Pi^*_{\overline{T}}(e_a)$, and for all $V = v_1\cdots v_n \in \mathcal{A}^*$, we set $w_V = \sum_{i=1}^n w_{v_i}$. With this notation,

$$\Pi^*Y^*(x) = \breve{\Pi}_s\Big(w_{P^W_{a_0}} + \sum_{i=0}^{N-1} A^{i+1}w_{P^*_i}\Big).$$

The final result relies on the following technical computation:

Lemma 7.3.

$$Aw_{P_0^*} + w_{P_{a_0}^W} - Aw_{P_{a_1}^W} = e_{\rho(P_0)} + e_{\rho(a_0)} - Ae_{\rho(a_1)}.$$

The proof consists in checking a finite number (16) of identities and is given in Section 9.3. We stress that it is purely computational and that we have still no (convincing) conceptual argument to guarantee such coincidence in a more general context. Now we use Lemma 7.3 inductively to show that for all N,

$$w_{P_{a_0}^W} + \sum_{i=0}^{N-1} A^{i+1} w_{P_i^*} = e_{\rho(a_0)} + \sum_{i=0}^{N-1} A^i e_{\rho(P_i)} + A^N(w_{P_{a_N}^W}) - A^N(e_{\rho(a_N)}).$$

We observe that $\breve{\Pi}_s A^N(w_{P_{a_N}^*}) \to 0$ and $\breve{\Pi}_s A^N(e_{\rho(a_N)}) \to 0$. Hence, taking the projection and letting N tend to infinity, we conclude that

$$\Pi^* Y^*(x) = \Pi^*\Big(\Pi^*_{T,u} e_{P_{a_0}^W} + \sum_{i=0}^{\infty} {}^t M^{-i-1} \Pi^*_{T,u} e_{P_i^*}\Big) = \breve{\Pi}_s e_{\rho(a_0)} + \sum_{i=0}^{\infty} A^i \breve{\Pi}_s e_{\rho(P_i)}.$$

So the claim is proved.

We already know (by a simple adaptation of Corollary 4.2) that the image of $\Pi \circ Y$ is the tribonacci fractal; hence, since $\mathcal{R}_W^* = \Pi^* Y^*(\mathbb{S}^1)$, the theorem is proved as well. □

8. ADDITIONAL REMARKS

8.1. Surface Diffeomorphisms

We have not considered here the pseudo-Anosov map that is associated with this interval-exchange transformation. Let us just remark here that the points α_i appear naturally in this setting as singular points on the surface, and the intervals K_i as initial segments of separatrices at the singularity. The pseudo-Anosov map preserves the singularity, but exchanges the separatrices. This helps to explain why it is reasonable to consider the interval exchange as defined, not on a circle, but on the union of three segments; it is just by coincidence that the endpoints of these segments turn out to be on the same orbit of the vertical flow, so that we can identify the extremities of the segments by sliding them along vertical orbits, and obtain a circle transverse to the vertical flow.

The interval exchange is measurably isomorphic to the substitution dynamical system associated with the tribonacci substitution; in this respect, tribonacci substitution seems linked to an automorphism of surfaces. However, as several people have noticed, there seems to be a contradiction here: every diffeomorphism of surfaces with orientable invariant foliation (this is the case here) has a homology matrix with a reciprocal characteristic polynomial, since it preserves the intersection form; but this is not the case for the tribonacci substitution. This was a starting point for this research, and the answer is that the tribonacci partition is not generating; the finer partition we found gives a substitution that factors on tribonacci substitution, and whose polynomial is generating.

In this particular case, it happens that we get the same fractal sets for the expanding and contracting directions; it is unclear whether this holds for all reciprocal substitutions, or at least for all substitutions associated with self-induced interval exchanges.

The sets K_i can be interpreted easily in the symbolic system, and also on the flat surface, as three segments of separatrices near a singular point. But they also appear, by projection onto the stable space $E_{T,s}$, as a partition of the tribonacci fractal, and the corresponding sets seem to tile the plane. Is such really the case, and what is the meaning of the corresponding lattice?

8.2. Duality and Higher-Dimensional Objects

In the present example, we were able to recover a dual substitution, because we knew the underlying interval exchange. It remains to find a general theory that allows one, when possible, to build a dual substitution. A dual substitution, which acts on faces of codimension 1, has been defined in [Arnoux and Ito 01]; but its relation to the substitution built here is not clear.

A general notion of higher-dimensional extensions of substitutions and their dual maps has been defined in [Arnoux et al. 01], and used in [Arnoux et al. 02, Arnoux et al. 04]. It would seem natural to use it in this framework to approximate the stable and unstable spaces; the fact that the present substitution is reducible, and the existence of a nontrivial neutral space, would probably make things more difficult for the present example. Note that some progress has been made recently on group automorphisms and associated tilings.

There is a symbolic dynamical system naturally associated with a substitution; in the basic examples (Pisot irreducible substitutions), this symbolic dynamical system has a symbolic representation as an exchange of pieces, which turns out in all known cases to be a translation on

a torus. In this paper, we have given another representation as an interval exchange transformation (which is measurably conjugate to a rotation on a torus); the good notion to consider in more complicated cases (reducible or non-Pisot) is unclear; in some non-Pisot cases, it seems to be a pseudogroup of translations.

Remark 8.1. We already observed that the underlying GIFS had to be the same (double duality) up to translation vectors. These translation vectors depend on the prefixes (and hence on the order) and on the basis.

8.3. Bi-infinite Sequences

For the sake of simplicity, we have mainly used infinite sequences, but of course it might be more natural, if somewhat cumbersome, to use bi-infinite sequences. In that case, there are countably many infinite sequences that can be extended in several different ways on the left, and only a finite number of orbits that branch at some point, with sequences that have the same past and different futures (or the converse).

In the present case, these special sequences can be interpreted as the discontinuity points of the interval exchange, where the image of a point can be defined differently using continuity on the right and continuity on the left.

It would also be interesting to study the bi-infinite fixed points on the dual substitution; there seem to be 12 of them, twice as many as for the initial substitution.

8.4. A More Symmetric Version

Increasing the number of letters, we can find another partition corresponding to another substitution:

$$\begin{aligned}
\sigma_s : 1_A &\to 2_B 3_A 3_B 4_A \\
1_B &\to 4_B 5_A 5_B \\
2_A &\to 6_A 6_B 1_A \\
2_B &\to 1_B 2_A \\
3_A &\to 1_A \\
3_B &\to 1_B \\
4_A &\to 2_A \\
4_B &\to 2_B \\
5_A &\to 3_A \\
5_B &\to 3_B \\
6_A &\to 4_A \\
6_B &\to 4_B .
\end{aligned}$$

Of course, the abelianization map has a three-dimensional null space, showing that nothing new happens, but this recoding may be useful in that it stresses better the symmetries. The correspondence is

$$1 \approx 1_A,\ 2 \approx 1_B,\ 3 \approx 2_A,\ 4 \approx 2_B,\ 5 \approx 3_A 3_B,\ 6 \approx 4_A,$$
$$7 \approx 4_B,\ 8 \approx 5_A 5_B,\ 9 \approx 6_A 6_B .$$

9. APPENDIX

9.1. Abelianization

The matrix of the substitution σ in the canonical basis is

$$M = M_\sigma = \begin{pmatrix}
0&0&0&1&1&1&0&0&0\\
0&0&0&0&0&0&1&1&0\\
1&0&0&0&0&0&0&0&1\\
0&1&1&0&0&0&0&0&0\\
1&1&0&0&0&0&0&0&0\\
0&0&1&0&0&0&0&0&0\\
0&0&0&1&0&0&0&0&0\\
0&0&0&0&1&0&0&0&0\\
0&0&0&0&0&1&1&0&0
\end{pmatrix}.$$

We choose a new basis $\widetilde{\mathcal{B}} = \{\tilde{e}_i, i = 1, \dots, 9\}$ adapted to the decomposition $\mathbb{R}^{\mathcal{A}} = E_n \oplus E_T \oplus E_{\overline{T}}$. Since these subspaces are given by rational equations, it is possible to choose vectors with integral coordinates (while it is not possible for the finer decomposition in stable and unstable spaces, because this finer decomposition is not given by rational equations); there are many possible choices. For convenience in computations, we will use half-integers. We denote by P the change of basis; its column vectors are the coordinates, in the canonical basis, of the vectors of the new basis:

$$P = \frac{1}{2}\begin{pmatrix}
0&0&0&0&2&0&1&0&-1\\
2&0&0&-1&-1&1&0&0&1\\
-2&0&0&1&-1&1&0&1&0\\
0&0&0&0&0&-2&1&-1&0\\
0&2&0&1&-1&1&0&1&0\\
0&-2&0&1&1&-1&0&0&1\\
0&0&0&-2&0&0&0&1&-1\\
0&0&2&1&1&-1&0&0&1\\
0&0&-2&-1&-1&1&0&0&1
\end{pmatrix}.$$

If $J = \begin{pmatrix} 0&0&1\\ 1&0&0\\ 0&1&0 \end{pmatrix}$ denotes the permutation matrix, and $A = \begin{pmatrix} 1&1&1\\ 1&0&0\\ 0&1&0 \end{pmatrix}$ the tribonacci matrix, then the matrix $\widetilde{M}$ corresponding to M in the new basis can be written as

$$\widetilde{M} = P^{-1}MP = \begin{pmatrix} J & 0 & 0\\ 0 & {}^tA^{-1} & 0\\ 0 & 0 & A \end{pmatrix}.$$

9.2. Arithmetic Basis

To give an arithmetic interpretation of the projections of the stepped line onto the subspaces E_n and $E_{\overline{T}}$, we consider another basis $\hat{\mathcal{B}}$ of these subspaces that allows us to recover the arithmetic properties of the IET.

Namely, we look for a projection onto a suitable subspace, and a basis of this subspace, such that the coordinates of the projections of the vectors of the canonical basis in this basis correspond to the coordinates in the natural basis of $\mathbb{Z}[\alpha]$ of the corresponding translations for the interval exchange transformation. It is in fact convenient to define this basis on the complete space $\mathbb{R}^{\mathcal{A}}$.

We define the basis $\hat{\mathcal{B}}$ by its coordinates in the canonical basis by the matrix

$$\hat{P} = \frac{1}{12}\begin{pmatrix} 0&0&0&-6&0&-6&6&0&-6\\ 6&10&-2&3&3&3&0&0&6\\ -6&-10&2&-3&-3&3&0&6&0\\ 0&0&0&6&0&0&6&-6&0\\ 6&4&4&-3&-3&3&0&6&0\\ -6&-4&-4&-3&-3&-3&0&0&6\\ 0&0&0&6&6&0&0&6&-6\\ 6&4&-2&-3&-3&-3&0&0&6\\ -6&-4&2&3&3&3&0&0&6 \end{pmatrix}.$$

The first vector $\hat{e}_1$ is the invariant vector, the first three vectors $\hat{e}_1, \hat{e}_2, \hat{e}_3$ form a basis $\hat{\mathcal{B}_N}$ of E_n; the next three vectors $\hat{e}_4, \hat{e}_5, \hat{e}_6$ form a basis $\hat{\mathcal{B}_{\overline{T}}}$ of $E_{\overline{T}}$, and the last three form a basis of E_T (these last three vectors are not changed from the basis $\widetilde{\mathcal{B}}$, and will play no role in what follows).

Definition 9.1.

1. We denote by F the subspace generated by $\hat{e}_1 - \hat{e}_4, \hat{e}_2 - \hat{e}_5, \hat{e}_3 - \hat{e}_6, \hat{e}_7, \hat{e}_8, \hat{e}_9$.
2. We denote by Π_F the projection onto $E_{\overline{T}}$ along F.
3. We denote by $\Pi_{E_j \oplus E_{\overline{T}}}$ the projection onto the subspace $E_j \oplus E_{\overline{T}}$ along the subspace $E_I \oplus E_T$.
4. We define the map $\hat{\Pi} = \Pi_F \circ \Pi_{E_j \oplus E_{\overline{T}}}$.

The map $\hat{\Pi}$ is a projection; direct computation shows that it is a projection onto $E_{\overline{T}}$ along the space generated by $\{\hat{e}_1, \hat{e}_2 + \hat{e}_4 - \hat{e}_5, \hat{e}_3 - \hat{e}_6, \hat{e}_7, \hat{e}_8, \hat{e}_9\}$, which allows us to recover its matrix:

Lemma 9.2. *If we consider the projection $\hat{\Pi}$ as a map from $\mathbb{R}^{\mathcal{A}}$, with the canonical basis $\mathcal{B}$, to $E_{\overline{T}}$, with the basis $\{\hat{e}_4, \hat{e}_5, \hat{e}_6\}$, its matrix is*

$$\begin{pmatrix} -1&-1&1&1&-1&-1&1&2&0\\ 1&1&-1&-1&0&0&0&-1&1\\ 0&0&0&0&1&-1&-1&-1&1 \end{pmatrix}.$$

Recall that for a 3-dimensional space E with a basis $\mathcal{B}$, we denote by $Q_{E,\mathcal{B}}$ the map defined on the lattice generated by $\mathcal{B}$ by $Q_{E,\mathcal{B}}(v) = \frac{n}{2} + \frac{p}{2}\alpha + \frac{q}{2}\alpha^2$, where (n, p, q) are the coordinates of v in the basis $\mathcal{B}$.

The essential result of this section is the following lemma:

Lemma 9.3. *The projections onto $E_{\overline{T}}$ of the canonical vectors satisfy*

$$Q_{E_{\overline{T}},\hat{\mathcal{B}}}(\hat{\Pi}(e_i))) = t_i.$$

Proof: This is a direct application of the previous lemma; we observe that applying Q to the matrix above, we obtain exactly the displacement vector

$$\frac{1}{2}\big(\alpha - 1, \alpha - 1, 1 - \alpha, 1 - \alpha, \alpha^2 - 1, -1 - \alpha^2, 1 - \alpha^2, 2 - \alpha - \alpha^2, \alpha + \alpha^2\big).$$

□

Remark 9.4. This lemma makes all further computations straightforward; it makes clear the link between what happens in the symbolic space and the more arithmetic description of the system.

There is a simple description of the projection $\hat{\Pi}$. Note that the projection Π_F is the identity on $E_{\overline{T}}$, the zero map on E_T, and that it sends E_n to $E_{\overline{T}}$ by a map that sends $\hat{e}_i$ to $\hat{e}_{i+3}$, for $i = 1, 2, 3$.

We can describe $\tilde{\Pi}$ simply by an abuse of language: let us identify E_n (with basis $\{\hat{e}_1, \hat{e}_2, \hat{e}_3\}$) and $E_{\overline{T}}$ (with basis $\{\hat{e}_4, \hat{e}_5, \hat{e}_6\}$) with $\mathbb{R}^3$ with the canonical basis, so that it makes sense to add vectors in these two different

$a_0 \to a_1$	$\rho(a_0)^{\rho(P_0)}_{\to}\rho(a_1)$	$\sigma_*(P_0^W)P_0^*$	$w_{a_0}+$	$Aw_{P_0^*}-$	$A(w_{a_1})=$	$e_{\rho(P_0)}+$	$e_{\rho(a_0)}-$	$Ae_{\rho(a_1)}=$	
$3 \to 9$	$a \xrightarrow{\epsilon} c$	$\sigma_*(\epsilon)\epsilon = \epsilon$	0	0	0	0	e_a	Ae_c	0
$3 \to 1$	$a \xrightarrow{\epsilon} a$	$\sigma_*(\epsilon)9$	0	Aw_9	Aw_{34}	0	e_a	Ae_a	$-e_b$
$4 \to 2$	$a \xrightarrow{\epsilon} a$	$\sigma_*(3)\epsilon$	w_3	$A0$	Aw_{341}	0	e_a	Ae_a	$-e_b$
$4 \to 3$	$a \xrightarrow{\epsilon} a$	$\sigma_*(3)2$	w_3	Aw_2	0	0	e_a	Ae_a	$-e_b$
$1 \to 4$	$a \xrightarrow{\epsilon} a$	$\sigma_*(34)\epsilon$	w_{34}	0	Aw_3	0	e_a	Ae_a	$-e_b$
$1 \to 5$	$a \xrightarrow{\epsilon} b$	$\sigma_*(34)4$	w_{34}	Aw_4	Aw_{67}	0	e_a	Ae_b	$-e_c$
$1 \to 6$	$a \xrightarrow{\epsilon} b$	$\sigma_*(34)45$	w_{34}	Aw_{45}	0	0	e_a	Ae_b	$-e_c$
$2 \to 7$	$a \xrightarrow{\epsilon} b$	$\sigma_*(341)\epsilon$	w_{341}	0	Aw_6	0	e_a	Ae_b	$-e_c$
$2 \to 8$	$a \xrightarrow{\epsilon} c$	$\sigma_*(341)7$	w_{341}	Aw_7	Aw_9	0	e_a	Ae_c	0
$6 \to 3$	$b \xrightarrow{a} a$	$\sigma_*(3412)\epsilon$	0	0	0	e_a	e_b	Ae_a	0
$7 \to 4$	$b \xrightarrow{a} a$	$\sigma_*(34126)\epsilon$	w_6	0	Aw_3	e_a	e_b	Ae_a	0
$5 \to 1$	$b \xrightarrow{a} a$	$\sigma_*(341267)\epsilon$	w_{67}	0	Aw_{34}	e_a	e_b	Ae_a	0
$5 \to 2$	$b \xrightarrow{a} a$	$\sigma_*(341267)1$	w_{67}	Aw_1	Aw_{341}	e_a	e_b	Ae_a	0
$9 \to 6$	$c \xrightarrow{a} b$	$\sigma_*(3412675)\epsilon$	0	0	0	e_a	e_c	Ae_b	0
$9 \to 7$	$c \xrightarrow{a} b$	$\sigma_*(3412675)6$	0	Aw_6	Aw_6	e_a	e_c	Ae_b	0
$8 \to 5$	$c \xrightarrow{a} b$	$\sigma_*(34126759)\epsilon$	w_9	0	Aw_{67}	e_a	e_c	Ae_b	0

TABLE 1. The 16 cases corresponding to the 16 edges of the prefix automaton.

spaces. Consider Π_j as a map from $\mathbb{R}^{\mathcal{A}}$ to $\mathbb{R}^3$, and $\Pi_{\overline{T}}$ also as a map from $\mathbb{R}^{\mathcal{A}}$ to $\mathbb{R}^3$.

The very definition of $\hat{\Pi}$ shows that with this abuse of language, we have

$$\hat{\Pi}(V) = \Pi_{\overline{T}}(V) + \Pi_j(V).$$

Since the projection Π_j takes only three values on the canonical stepped line, as we saw above, the difference between $\tilde{\Pi}$ and $\Pi_{\overline{T}}$ on the canonical line also can take only three values; the McMullen curve differs from the standard projection of the canonical line on $E_{\overline{T},u}$ by a finite set of translations.

9.3. Proof of Lemma 7.3

Let us do the complete computation to show that $Aw_{P_0^*} + w_{P^W_{a_0}} - Aw_{P^W_{a_1}} = e_{\rho(P_0)} + e_{\rho(a_0)} - Ae_{\rho(a_1)}$. We recall that w_a stands for $\Pi\Pi^*_{\overline{T}}(e_i)$. We observe that $E^*_{\overline{T}}$ is indeed determined by the system of linear equations

$$\begin{aligned} w_1 + w_2 + w_3 + w_4 &= 0,\\ w_5 + w_6 + w_7 &= 0,\\ w_8 + w_9 &= 0,\\ w_2 + w_6 &= 0,\\ w_6 - w_8 &= 0,\\ w_3 - w_5 &= 0. \end{aligned}$$

It is hence clear that $e_a = -w_7, e_b = w_1$ and $e_c = -w_4$ is a basis. We recall that in this basis, the restriction of ${}^tM^{-1}$ acts as the tribonacci matrix A. The other vectors are

$$\begin{aligned} w_2 &= \frac{1}{2}(-e_a - e_b + e_c),\\ w_3 &= \frac{1}{2}(e_a - e_b + e_c),\\ w_5 &= \frac{1}{2}(e_a - e_b + e_c),\\ w_6 &= \frac{1}{2}(e_a + e_b - e_c),\\ w_8 &= \frac{1}{2}(e_a + e_b - e_c),\\ w_9 &= \frac{1}{2}(-e_a - e_b + e_c). \end{aligned}$$

The 16 cases corresponding to the 16 edges of the prefix automaton are listed in Table 1.

REFERENCES

[Arnoux 88] P. Arnoux. "Un exemple de semi-conjugaison entre un échange d'intervalles et une translation sur le tore" (An Example of Semiconjugacy between an Interval Exchange and a Shift on the Torus). *Bull. Soc. Math. France* 116;4 (1988), 489–500.

[Arnoux and Ito 01] P. Arnoux and S. Ito. "Pisot Substitutions and Rauzy Fractals." *Bull. Belg. Math. Soc. Simon Stevin* 8 (2001), 181–207.

[Arnoux and Yoccoz 81] P. Arnoux and J.-C. Yoccoz. "Construction de difféomorphismes pseudo-Anosov." *C. R. Acad. Sci. Paris, Sér. I Math.* 292;1 (1981), 75–78.

[Arnoux et al. 01] P. Arnoux, S. Ito, and Y. Sano. "Higher Dimensional Extensions of Substitutions and Their Dual Maps." *Journal d'Analyse Mathématique* 83 (2001), 183–206.

[Arnoux et al. 02] P. Arnoux, V. Berthé, and S. Ito. "Discrete Planes, $\mathbb{Z}^2$-Actions, Jacobi-Perron Algorithm and Substitutions." *Ann. Inst. Fourier (Grenoble)* 52 (2002), 1001–1045.

[Arnoux et al. 04] P. Arnoux, V. Berthé, and A. Siegel. "Two-Dimensional Iterated Morphisms and Discrete Planes." *Theoret. Comput. Sci.* 319 (2004), 145–176.

[Bowman 08] J. Bowman. "Orientation-Reversing Involutions of the Genus 3 Arnoux–Yoccoz Surface and Related Surfaces." arXiv:0812.3144v1, 2008.

[Dumont and Thomas 93] J.-M. Dumont, and A. Thomas. "Digital Sum Moments and Substitutions." *Acta Arith.* 64:3 (1993), 205–225.

[Fathi 88] A. Fathi. "Some Compact Invariant Sets for Hyperbolic Linear Automorphisms of Tori." *Ergod. Th. and Dynam. Sys.* 8 (1988), 191–204.

[Fogg 02] N. Pytheas Fogg. *Substitutions in Dynamics, Arithmetics and Combinatorics,* Lecture Notes in Mathematics 1794. New York: Springer-Verlag, 2002.

[Hubert and Lanneau 06] P. Hubert and E. Lanneau. "Veech Groups without Parabolic Elements." *Duke Math. J.* 133 (2006), 335–346.

[Hubert et al. 09] P. Hubert, E. Lanneau, and M. Möller. "The Arnoux–Yoccoz Teichmüller Disc." *Geom. Funct. Anal.* 18;6 (2009) 1988–2016.

[Lowenstein et al. 07] J. H. Lowenstein, G. Poggiaspalla, and F. Vivaldi. "Interval Exchange Transformations over Algebraic Number Fields: The Cubic Arnoux–Yoccoz Model." *Dyn. Syst.* 22;1 (2007), 73–106.

[McMullen 09] C. T. McMullen. Gallery. Available online http://www.math.harvard.edu/∼ctm/gallery/index.html/

[Messaoudi 00] A. Messaoudi. "Frontière du fractal de Rauzy et systéme de numération complexe." *Acta Arith.* 95:3 (2000), 195–224.

[Nipper 08] E. Nipper. "Minimality and Nonergodicity on a Family of Flat Surfaces in Genus 3." arXiv:0801.0466v1, 2008.

[Rauzy 82] G. Rauzy. "Nombres algébriques et substitutions." *Bull. S.M.F.* 110 (1982), 147–178.

[Sirvent 97] V. Sirvent. "Identifications and Dimension of the Rauzy Fractal." *Fractals* 5:2 (1997), 281–294.

[Sirvent 00] V. Sirvent. "Geodesic Laminations as Geometric Realizations of Pisot Substitutions." *Ergodic Theory Dynam. Systems* 20;4 (2000), 1253–1266.

Pierre Arnoux, Institut de Mathématiques de Luminy CNRS U.M.R. 6206, 163, avenue de Luminy, Case 907, 13288 Marseille Cedex 09, France (arnoux@iml.univ-mrs.fr)

Julien Bernat, IUFM de Lorraine et Institut Elie Cartan, CNRS U.M.R. 7502, Université Henri Poincarée Nancy 1, B.P. 239, F-54506 Vandoeuvre-lés-Nancy Cedex, France (julien.bernat@lorraine.iufm.fr)

Xavier Bressaud, Université Paul Sabatier, Institut de Mathématiques de Toulouse, F-31062 Toulouse Cedex 9, France (bressaud@math.univ-toulouse.fr)

Received November 9, 2008; accepted March 25, 2009.